Advanced Flexible Wing Technology Assessment for Transport Applications

by

Shawn J. Hanegan

S.B. Aeronautics and Astronautics

Massachusetts Institute of Technology, 1995

Submitted to the Department of Aeronautics and Astronautics in partial fulfillment of the requirements for the degree of

Master of Engineering

at the

MASSACHUSETTS INSTITUTE OF TECHNOLOGY

June 1996

Author .....
Department of Aeronautics and Astronautics
May 28, 1996

Certified by .....
Charles Boppe
Senior Lecturer, Department of Aeronautics and Astronautics
Thesis Supervisor

Certified by .....
Mark Drela
Associate Professor of Aeronautics and Astronautics
Thesis Supervisor

Accepted by .....
Harold Wachman
Chairman, Departmental Graduate Committee

Advanced Flexible Wing Technology Assessment for Transport Applications

by

Shawn Hanegan

Submitted to the Department of Aeronautics and Astronautics on
May 28, 1996, in partial fulfillment of the requirements for the
degree of Master of Engineering

Abstract

Issues involving the use of Advanced Flexible Wing (AFW) technology on a transport aircraft are examined. Four issues are looked at in depth: span efficiency, control effectiveness, reversal speed, and structural response. Results show wing flexibility can result in significant weight reduction. A baseline wing and flexible wing adaptations of the baseline wing are designed for use on Lockheed's New Strategic Airlifter (NSA). Requirements analysis of the NSA shows reduction of structural weight to be a primary design driver. Analysis of the NSA's intended functions reveals potential design variants concerning use of AFW. The process for designing a baseline wing involves taking Lockheed-specified requirements and derived requirements, based on analysis and empirical practice, and producing a wing design. Wing planform, structural layout, and mission profile are determined in this manner. Sizing of structural elements for the baseline wing is performed by the computer program ASTROS. Structural and aerodynamic properties are input into the computer code ASWING for sensitivity analysis. Torque box weight is reduced from the baseline wing case to produce flexible wing designs, with all other sizings being kept the same. At 24% reduction in total wing weight, the wing is at its yield point. No aileron reversal problems are associated with flexibility in this design. Control effectiveness does decrease markedly. Maintenance of span efficiency in a flexible wing requires the use of fixture built-in washin, which has the consequence of increasing shear stress.

Thesis Supervisor: Charles Boppe
Title: Senior Lecturer, Department of Aeronautics and Astronautics

Thesis Supervisor: Mark Drela
Title: Associate Professor, Department of Aeronautics and Astronautics

Acknowledgments

Carrying out the department's first Master of Engineering project was certainly a memorable experience, with all the ups and downs that came with it. I am glad to have partaken in it, and feel that what I learned will be valuable for me in the years to come as I enter into industry. I would like to thank the following people for enriching my experience.

First of all, I thank my parents for the love and support they have given me throughout my academic career.

I would also like to thank Charlie Boppe for his dedication to the MEng program and to our project. Charlie's long hours at work were appreciated.

I thank Terry Weisshaar for his support and advice throughout the term. As a visiting professor from Purdue, Terry had no obligations to become involved in our thesis, but yet chose to play a key role from the beginning.

I would also like to thank my teammate Jerry Wohletz for getting through this with me. He brought to the project a great deal of experience from the University of Kansas and from industry, experience that was vital to the work that was done. We also managed to have some fun times along the way.

I thank my friends whose zephyrs during the long hours I was at the computer working provided me with entertainment.

Finally, a great deal of gratitude is extended to Professor Mark Drela who was always willing to help when we needed him, including the one night he stayed up with us until 1:30 before a presentation in order to help us obtain all of the needed data. Mark put in quite a bit of time to modify his ASWING code to be able to be used in this project, without which we would not have been able to obtain many of our results.

Table of Contents

List of Figures

List of Tables

Chapter 1

Introduction and Background

1.1 Advanced Flexible Wing (AFW) Concept

Cost is becoming an increasingly important factor in aerospace vehicle design. An Advanced Flexible Wing, sometimes called an Active Flexible Wing, has been proposed as a design alternative that could potentially lead to lower vehicle cost through reductions in structural weight and at the same time improve aerodynamic efficiency and reduce control surface sizing.

Structural elements in a conventional wing are sized, in most cases, by stiffness constraints resulting from limits placed on torsional and bending deflections. An AFW differs from a conventional wing in that its torsional stiffness constraint is reduced. Lessening of the stiffness constraint can lead to significant structural weight reduction. Figure 1.1 is a schematic of where weight savings are applicable in terms of wing design parameters:

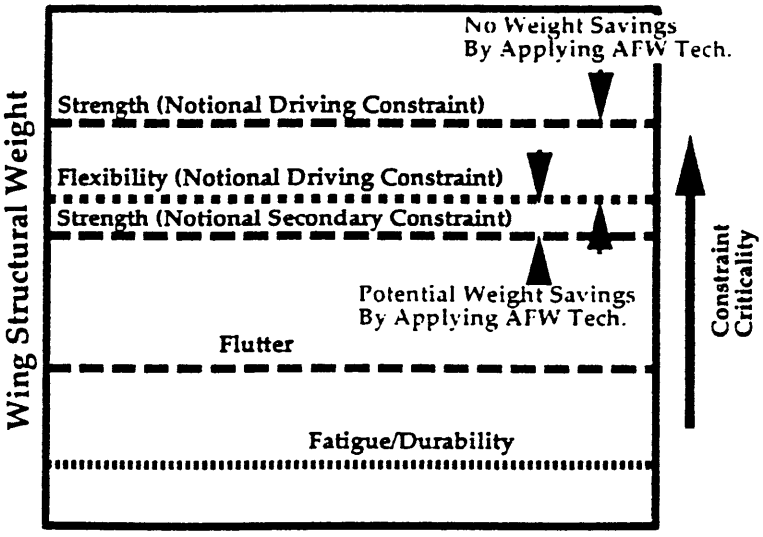

Figure 1.1: Relationship Between Wing Structural Weight Drivers (Ref. 1)

Wing flexibility can be used to generate roll control power and improve aerodynamic performance at off-design points (Ref. 1). Thus, an AFW potentially can lead to reductions in control surface size and complexity and an increase in control power. Because degree of flexibility can be controlled in an AFW, tailored aero efficiency increments and design parameter flexibility are also potential benefits. The control mechanisms expected to be employed on an AFW are shown in Figure 1.2.

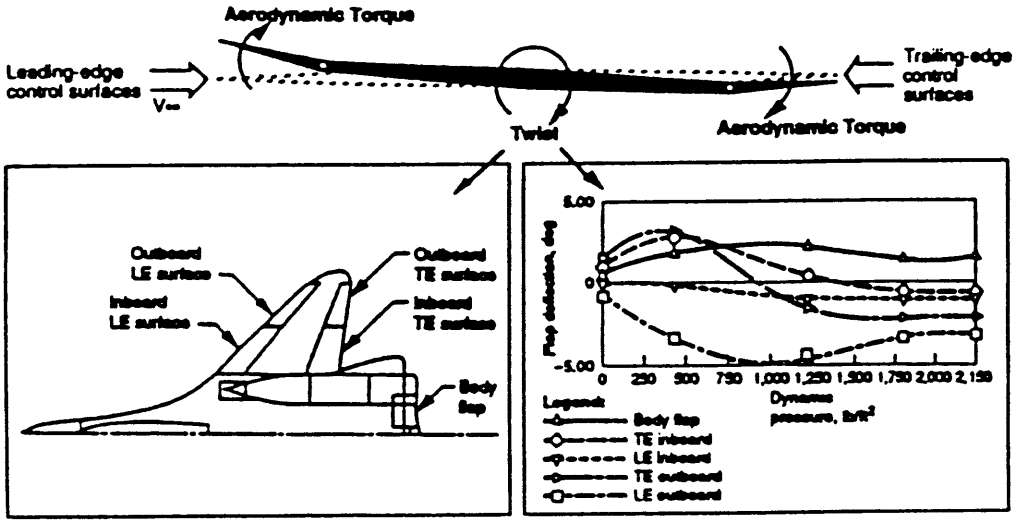

Figure 1.2: AFW Control Mechanisms (Ref. 1)

1.2 Previous AFW Work

1.2.1 Lockheed Martin and Rockwell

Lockheed Martin and Rockwell teamed up on a project to perform a feasibility study of the use of AFW technology for high performance fighter-type aircraft (Ref. 1). The aircraft used in the study was a single-engine, single-seat, conventional takeoff and landing generic strike fighter. Two wings, one AFW and one conventional wing, were designed around the same planform, thickness-to-chord ratio and control surface geometry. Major differences between the two wings were degree of flexibility and the control scheme used to vary camber and generate roll. Traditional control effectors were used in the conventional case, whereas the AFW design employed control tabs that take into account reversal phenomena, like those shown in Figure 1.2, in order to twist the

wing. Results of the study showed a potential reduction in gross takeoff weight of 7.1%, which led to an 8.7% reduction in empty weight savings. The majority of the weight savings was realized by reducing the wing structural weight. Structure, in the AFW case, was sized by a Mach 0.9 maneuver point and a Mach 1.5 excess power requirement. Areas of concern as quoted from Ref. 1 were:

- Structural impact of wing-mounted, bring-back payload during repeated carrier arresting operations
- Mechanical and structural feasibility of large tab deflections during high dynamic pressure operations
- Damage tolerance considerations

1.2.2 Wind Tunnel Tests at NASA-Langley

In 1991, a wind-tunnel model of an AFW was tested at NASA-Langley. Ref. 2 includes a discussion of several of these experiments. Two leading edge and two trailing edge control surfaces were used in the model. Key program accomplishments included:

- Single and multiple mode flutter suppression
- Load alleviation and load control during rapid roll maneuvers
- Multi-input, multi-output, multiple-function active control tests above the open-loop flutter boundary
- Testing process included methodology for successful on-line controller performance evaluation

1.3 Applications to New Strategic Airlifter

While previous work has identified possible benefits for use of an AFW on fighter-type aircraft, to the author's knowledge there is no existing study published on the use of an AFW on a transport aircraft. The goal of this project was to conduct a technology assessment of a high aspect ratio flexible wing for a transport aircraft. Project logistics are discussed in Appendix A.

The transport used for analysis was Lockheed's New Strategic Airlifter (NSA). The NSA is intended to be a cargo plane with both military and commercial applications. In order to determine AFW applicability to the design of this vehicle, a requirements analysis

was performed to identify customer needs and the potential effect that an AFW design might have in meeting these needs. Derived requirements were then determined with Lockheed-given parameters, engineering analysis, and best current practices in wing structural design. A baseline wing was designed for the NSA planform using computer analysis tools. Because of time limitations, only one design iteration was performed, however several potential design variants were identified for consideration in future projects. Using this baseline wing as a foundation, wings with increased flexibility were designed by reducing the weight of the baseline wing torque box. A sensitivity analysis on the effect of different torque box weight reductions on control effectiveness, span efficiency, and structural effects was performed. By comparing the resulting flexible wings with the stiffer baseline wing, a number of benefits were identified.

Chapter 2

Requirements Analysis

2.1 Significance

The primary purpose served by the requirements analysis process in this project was twofold. First, a basis was needed for the design of a baseline wing for the NSA. For this purpose, the requirements analysis process identified mission parameters, structural layout, planform geometry, and the effect of structural sizing on structural properties. Secondly, the requirements analysis process pointed out key areas where AFW technology is expected to impact wing design. Some of these areas were examined with the sensitivity studies in this project. Those areas not examined by this study represent potentially important future research on the subject of AFWs.

2.2 Customer Needs

An Operational Requirements Document (ORD) which describes intended functions and design requirements of the NSA was provided by Lockheed Martin. The ORD is attached as Appendix B. Analysis of this document combined with the use of empirical data from other sources led to a ranking of importance for each of the customer needs. While the ORD discusses five possible mission scenarios for the NSA, both military and commercial, it focuses on the military deployment mission, which is expected to be the determinate factor in the wing's structural design. Thus, the deployment mission was also the focus of this design.

2.2.1 Requirements Hierarchy

A requirements hierarchy was constructed from the ORD. Customer needs were separated into mission scenarios. Functional requirements were then extracted from the wording of the ORD. Functional requirements are defined as operational actions or activities needed to solve a customer problem, i.e. carry payload. One level below functions in the requirements hierarchy are requirement types, or function attributes. There are several different categories of requirement types (Ref. 3):

• performance requirements (measures of how well functions are performed)

• reliability requirements (measures of how well the functions are performed over time)

• maintainability (measures of how well the system can be fixed if failure occurs)

• extensibility (ability to adapt to new changes or requirements)

• constraints (factors that place limits on the design and may affect design trades between the other attributes)

By analyzing and subcategorizing the requirements, a hierarchy was constructed. Size of the hierarchy precludes inclusion of its entirety, but a portion is shown in Figure 2.1, which depicts a subset of the deployment mission requirements.

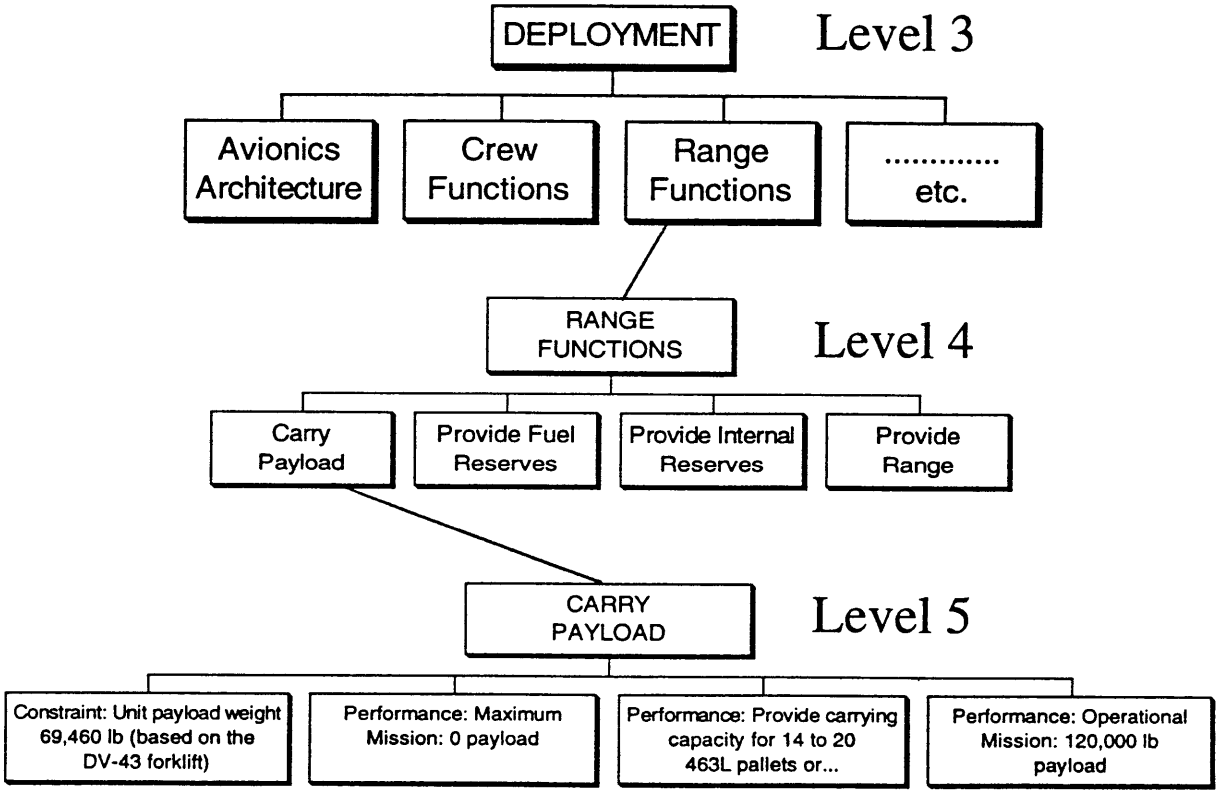

Figure 2.1: Requirements Hierarchy

2.2.2 Explicit Customer Needs

From the requirements hierarchy, explicit customer needs were identified and prioritized using an evaluation scheme based on the number of times a requirement was

mentioned and the importance given to it in each particular context. Table 2.1 is a list of some of the most important explicit customer needs and their respective rankings (10 being highest).

Table 2.1: Explicit Customer Needs

Ranking	Customer Need
10	Large Payload Capacity
10	Long Range
10	Reliability, Maintainability, and Supportability
7	Advanced Flight Management System
7	Survivability
4	High Speed
4	High Altitude

2.2.3 Implicit Customer Needs

A search was performed for requirements which pertain to customer needs, but were not explicitly stated in the ORD. For this project, the only implicit requirements fully examined were those that influence cost. Although the ORD never specifically mentioned cost, life cycle cost is now a critical requirement (and sometimes a constraint) in any military procurement program. It is also a primary factor in any commercial program as well. Reducing life cycle cost entails reducing direct operating cost (DOC) and acquisition cost. For this analysis, only DOC was subcategorized.

DOC was broken down into flying cost, maintenance cost, depreciation cost, and miscellaneous costs. A typical DOC breakdown for narrow-body transports is shown in Figure 2.2. Three planes were considered in making this calculation: MD-90-50, B737-300, and A320-200. DOC was computed for the following four ranges: 1000 nm, 1500 nm, 2000 nm, and 3000 nm. Results were averaged for each of the airplanes and for each of the ranges where applicable. Parameterized equations as cited in Ref. 4 were used to perform the calculations, with the key assumption being a $1 US per gallon fuel price.

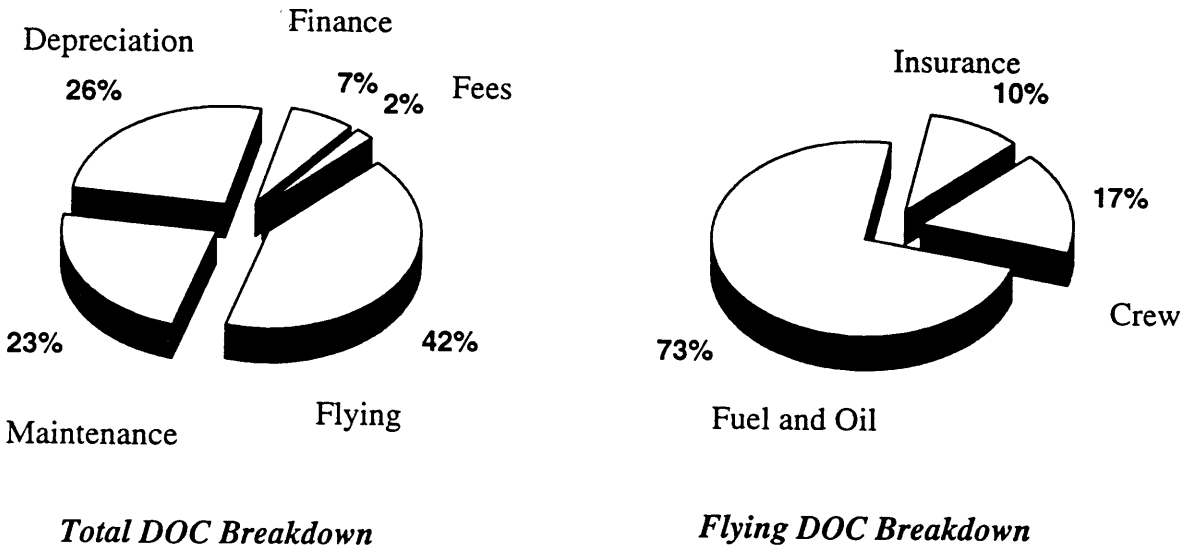

Figure 2.2: Typical DOC Breakdown (Ref. 5)

General trends of DOC for narrow-body commercial transports are representative of DOC general trends for military cargo planes, and were therefore judged applicable to the NSA design. A relationship matrix was developed which compares the effects of several technical requirements on each of the DOC drivers. Importance of each of the DOC drivers was represented as a direct percentage of their respective effects on DOC as shown in Figure 2.2. A list of typical design goals was examined to determine strength of effect, if any, each had on the DOC drivers. A quantitative evaluation of importance is assigned based on the sum of these effects. From the results of this matrix, implicit customer needs were identified and prioritized. These results are summarized in Table 2.2. The matrix itself is presented as Figure 2.3.

Table 2.2: Implicit Customer Needs

Ranking	Customer Need
10	Minimize Aircraft Weight
6	Minimize Aircraft Purchase Price
6	Minimize Block Fuel Consumption
6	Minimize Number of Engines
5	Minimize Maintenance Man-Hours
5	Minimize Depreciation

Quadratic Weights	
9	Strong Positive
3	Positive
1	Weak

			Minimize Block Fuel Consumption	Minimize Fuel Price	Maximize Fuel Density	Minimize Weight of Oils and Lubricants	Minimize Number of Engines	Minimize Annual Block Time	Maximize Oil/Lubricant Density	Minimize Oil/Lubricant Price	Minimize Number of Pilots/Crew	Minimize Aircraft Purchase Price	Maximize Annual Block Time	Maximize Block Speed	Minimize Flight Delays	Minimize Maintenance Man Hours	Minimize Labor Rate	Minimize Aircraft Weight	Minimize Takeoff Thrust	Minimize Engine Purchase Price	Maximize Time Between Engine Overhaul	Minimize Depreciation Rate	Maximize Number of Engines	Maximize Engine Price	Maximize Price Of Avionics	Maximize Depreciation Period	Maximize Block Time
Flying Cost	Minimize Fuel and Oil Cost	31	9	3	1	1	3	1	1	1								9									
	Minimize Crew Cost	7									9																
	Minimize Airframe Cost	4										9	3	3													
Maintenance Cost	Minimize Airframe/Systems Labor MC	5						3						1	1	9	3	9									
	Minimize Engine Labor MC	5					9	3						1	1	9	3	1	3								
	Minimize Airframe/Systems Materials MC	5										3		1	1	9		9									
	Minimize Engine Materials MC	5					9								1	9				9	9						
	Minimize Applied Materials MC	5					3	3				1		1	1	9	3	9	1	3	3						
Depreciation Cost	Minimize DC of Airplane without Engines	5										9		3								9	1	1	1	9	3
	Minimize DC of Engine	5					9					9		3								9				9	3
	Minimize DC of Avionics Systems	5										9		3								9				9	3
	Minimize DC Airplane Spare Parts	5										3		3								9	1	1		9	3
	Minimize DC Engine Spare Parts	5					3					3		3								9				9	3
Other Cost	Minimize Landing Fees	1												3				9									3
	Minimize Registry Taxes	1																9									
	Minimize Financing Cost	7										9															
			279	93	31	31	258	76	31	31	63	284	12	110	25	225	45	437	20	60	60	225	10	10	5	225	78
			6	2	1	1	6	2	1	1	1	6	0	3	1	5	1	10	0	1	1	5	0	0	0	5	2

Figure 2.3: DOC Relationship Matrix

Implicit and explicit customer needs were then combined into an overall ranking. Weightings of implicit customer needs reflect the prioritization obtained from the DOC relationship matrix with one exception. Because of the importance of acquisition cost, aircraft purchase price was given the same priority as minimization of takeoff weight; in fact the two are inherently related. Table 2.3 shows a listing of these weightings, subcategorized into three types.

Table 2.3: Explicit and Implicit Customer Needs

Cost Drivers:

Ranking	Customer Need
10	Minimize Aircraft Takeoff Weight
10	Minimize Aircraft Purchase Price
7	Minimize Block Fuel Consumption
7	Minimize Number of Engines
6	Minimize Maintenance Man-Hours
6	Minimize Depreciation

Operational Drivers

10	Reliability, Maintainability, and Supportability
7	Advanced Avionics
7	Survivability

Performance Drivers

10	Large Payload Capacity
10	Long Range
4	High Speed
4	High Altitude
4	Long Endurance

2.2.4 QFD analysis

Quality Functional Deployment (QFD) is a technique used to assign weightings to technical requirements based on their relative importance in meeting customer needs. A QFD requirements matrix, or "House of Quality" is developed in order that a quantitative value may be computed for each design parameter. Figure 2.4 illustrates the concept.

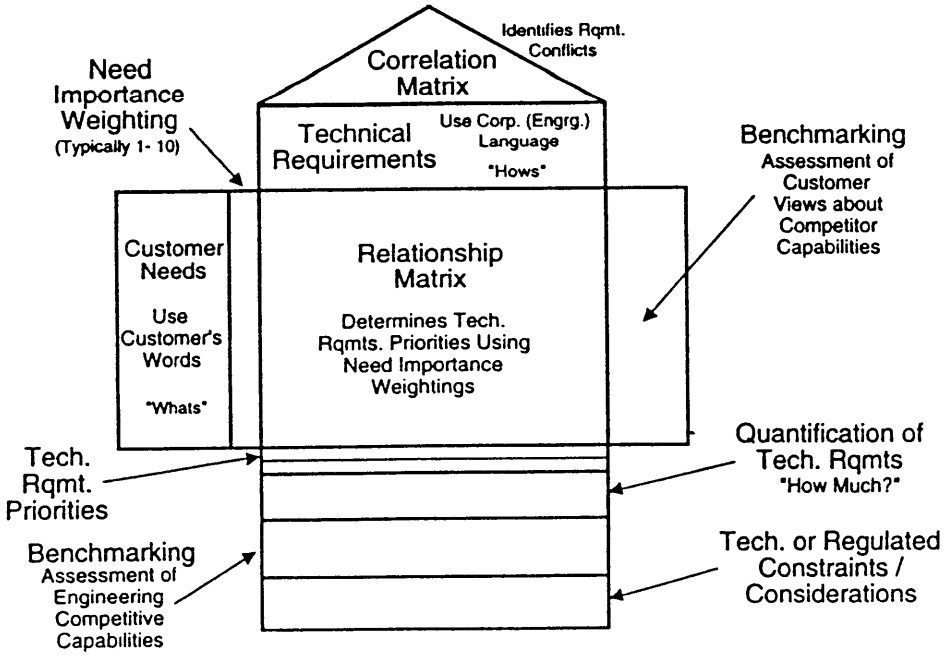

Figure 2.4: QFD concept (Ref. 6)

Technical requirements are compared against customer needs. The relationship matrix, like the DOC relationship matrix in Figure 2.3, assigns weighting terms to technical requirements based on the degree of influence each requirement has in terms of meeting a particular customer need. Several different weighting schemes are available. In this particular design, traditional practice was altered and penalties were assigned for negative effects. It was the author's decision that this method would produce more realistic results. Weighting numbers in the relationship matrix are multiplied by the customer need importance weightings in order to arrive at technical requirement priorities. The "roof" on the house is a correlation matrix which identifies those technical requirements that conflict with others. For example, if "minimizing structural weight" and "increasing aspect ratio" were two design goals, achieving one would make the other one harder to achieve. This conflict would be noted in the correlation matrix. Such conflicts are used to identify where design trade studies should be performed. For this design the perimeter comment regions are not used. A detailed description of the QFD process is given by Ref. 6.

The QFD build for the NSA wing design is shown by Figure 2.5. For clarity, technical requirements were subdivided into seven categories: weight, aerodynamic efficiency, engine efficiency, engine sizing, manufacturing, technology, and support. Also, customer needs were categorized into three types: cost, performance, and support (operational) drivers. From the resultant QFD build, a set of prioritized technical requirements was determined, and is shown in Table 2.4.

2.2.5 Customer Needs Summary

Through breakdown of the ORD, explicit customer needs were obtained. Implicit customer needs were identified based on life cycle cost design drivers. Both explicit and implicit customer needs were then assimilated and prioritized. Technical requirements were identified and prioritized through the QFD process based on their impact on important customer needs.

Quadratic Weights	
9	Strong Positive
3	Positive
1	Weak
-3	Negative
●	Conflict

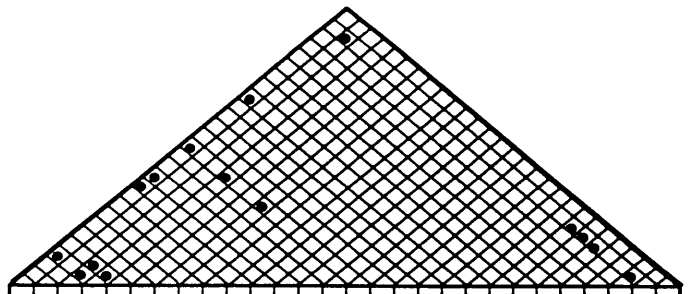

			Minimize Structural Weight	Reduction in System and/or Synergize	Maximize Cruise Lift to Drag Ratio	Aspect Ratio	Optimized Cruise Lift Distribution	Minimize Surface Area	Bypass Ratio	Turbine Inlet Temperature	Tip Clearance	Minimize Number of Engines	Maximize Takeoff T/W	Maximize Sea-Level Thrust	Maximize Lift Coefficient	Maximize Wing Loading	High Cruise Mach Number	Design for Manufacturing	Design for Assembly	Commercial Practices	Reduce Part Count	Number of Different Materials	Advanced Materials	Advanced Avionics	Advanced Manufacturing Process	High Reliability Components	Ergonomic Design	Modular Design	Systems Commonality	Standards Ground Equipment
			We		Aero Eff.				Eng. Eff.			Engine Sizing						Manufacturing					Tech.			Support					
Cost Drivers	Minimize Aircraft Takeoff Weight	10	9	3	3	1	3	1				9	-3			3					3		9	3						
	Minimize Aircraft Purchase Price	10	9	3								9						9	9	9	9	1	-3	-3	9			3	9	
	Minimize Block Fuel Consumption	7	9		9	9	9	9	9	3	3	3	3	-3			-3						3							
	Minimize Number of Engines	7	9	1	3				3	3	3	9	-3	3	9	9	-3													
	Minimize Maintenance Man Hours	6	3	9								9						1	1		3	3	-3	9	1	9	9	9	9	9
	Minimize Depreciation	6	9	9								9					9	9	9	3	1		9	9	9	9	1	9	1	1
Performance	Large Payload Capacity	10	9	3	3	1						1	9	9	9								3							
	Long Range	10	3	1	9	9	9	9	9	1	1		-3	-3								1	3							
	High Speed	4	-3	1	9			3	-3				3	3			9													
	High Altitude	4	3	1	9	9	3	1	3				3	3			3													
	Long Endurance	4	3	1	9	9	9	9	3	1	1		-3	-3			-3												3	
Support	Reliability, Maintainability, & Supportability	10	3	9														9	9		9	9	-3	9		9	9	9	9	9
	Advanced Flight Management System	7																						9		9		3		
	Survivability	4	3	-3								-3	9	9	9		9									9		-3		
			552	305	342	245	231	215	186	56	56	370	78	108	189	93	84	240	240	108	244	118	147	261	150	297	150	237	252	150

Figure 2.5: QFD Build.

Table 2.4: Prioritized Technical Requirements

Wing Structural Weight

10	Minimize Structural Weight
6	Reduction in Systems and/or Synergize
6	Maximum Cruise L/D
4	Maximize Aspect Ratio
4	Optimize Cruise Lift Distribution
4	Minimize Surface Area

Aerodynamic Efficiency

6	Maximize Cruise L/D
4	Maximize Aspect Ratio
4	Optimize Cruise Lift Distribution
4	Minimize Surface Area

Reliability, Maintainability, and Supportability

5	Highly Reliable Components
5	System Commonality
4	Reduce Parts Count
4	Design for Manufacturing and Assembly
4	Modular Design

2.3 Baseline Configuration

Figure 2.6 shows a three-view of the Lockheed-provided baseline configuration for the NSA. The three-view shows planform sizing and engine placement. The same configuration was used for the baseline wing and all of the flexible variants used in this project.

2.4 Derived Requirements

Beyond customer needs, the ORD was examined for technical flight requirements. Using ORD explicit specifications and empirical practice, a set of derived requirements was obtained for the deployment mission of the NSA. Derived requirements represent the mission profile (used for determining loads), structural arrangement and structural properties (used for sizing of structural elements). These derived requirements, along with the baseline configuration, are used in the design of a baseline wing for the NSA.

2.4.1 V-n Diagram

The limit loading during flight for a plane in the weight category of NSA is 2.5 g (Ref. 7). Gross takeoff weight is specified as 400,000 lbs. Initial cruise weight is therefore 380,000 lbs. (-5% of original fuel mass) Cruise altitude is 32,000 feet with a Mach number

of 0.82. A V-n diagram was prepared which represents the worst-case combined weight and dynamic pressure flight scenario. The diagram is shown in Figure 2.7. This type of diagram shows the combined velocity and loading conditions that the aircraft is expected to withstand during the worst-case scenario maneuver. However, the V-n diagram resulted from consideration of only one point in the flight envelope, and only 6 loading scenarios out of a possible 38 listed in Ref. 8 were considered.

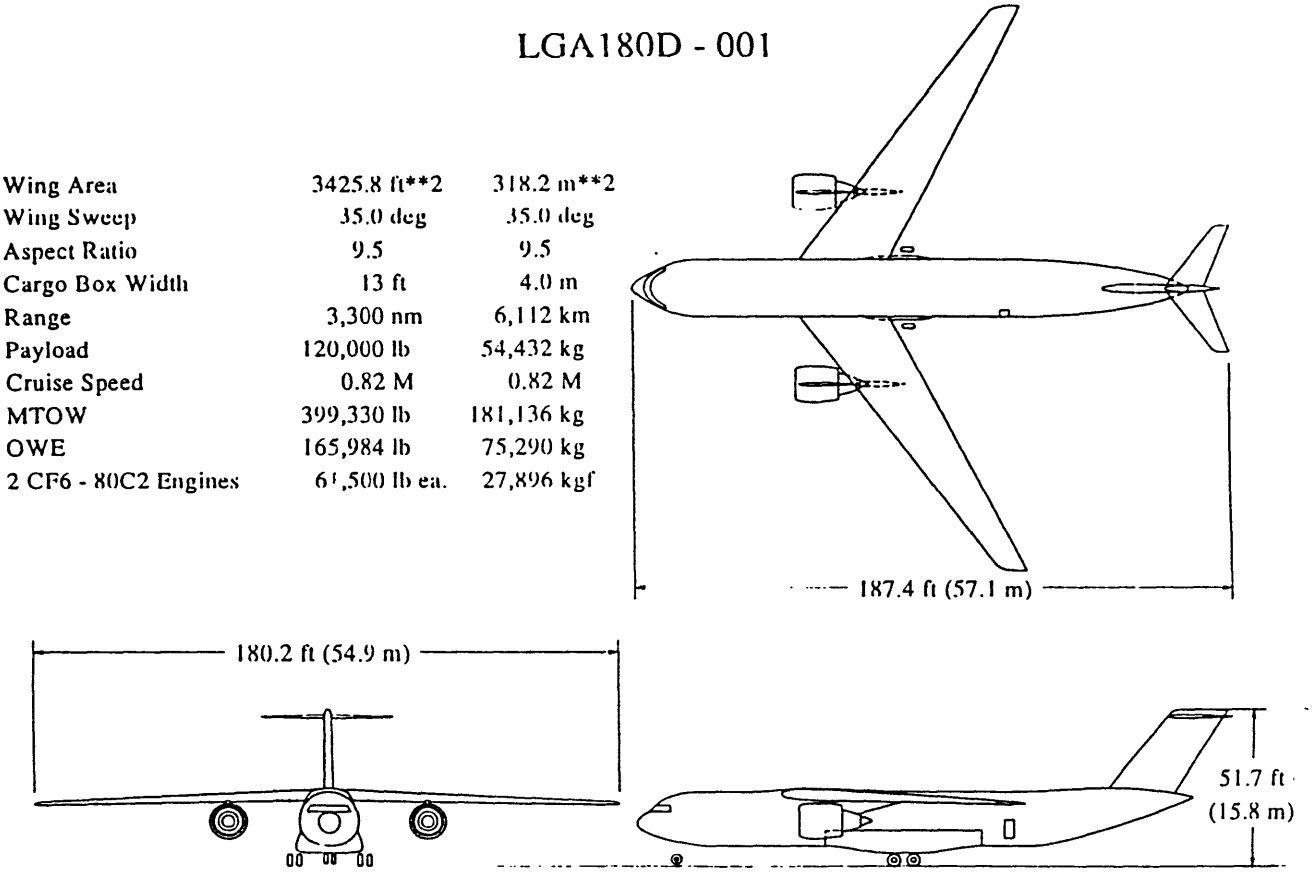

Figure 2.6: Baseline Configuration

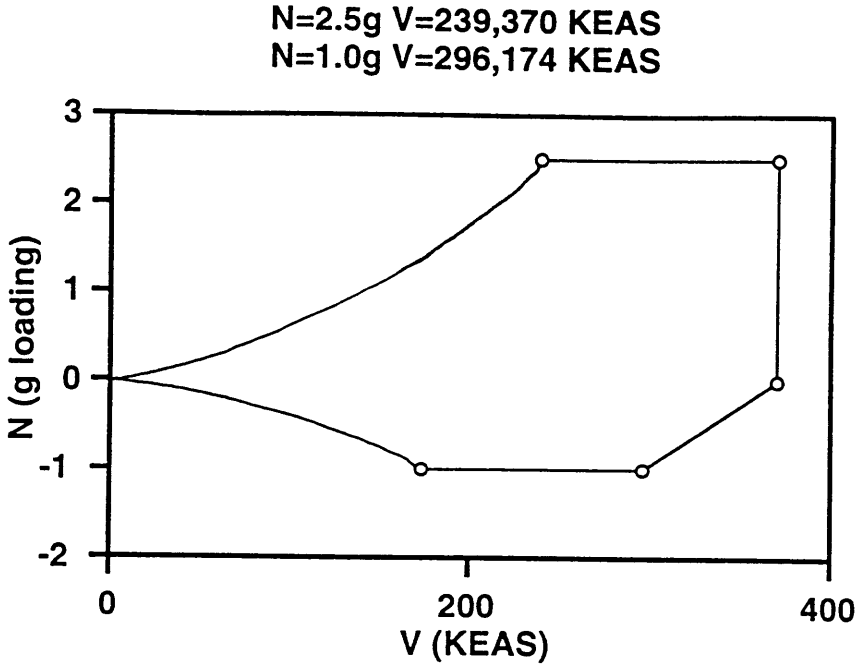

Figure 2.7: V-n diagram

2.4.2 Wing Structural Arrangement and Material Selection

For this design, a two spar wing was chosen with the front spar placed at 15% of the chord and the rear spar placed at 65%, measurements taken perpendicular to the mid-point of the chord. A generic supercritical airfoil was used. Airfoil and spar locations are shown in Figure 2.8.

Figure 2.8: Airfoil Shape with Spar Locations

Rib spacing was usually set at 24 inches. Unless obstructed by a pylon, stringers were spaced every 12 inches starting from the trailing edge of the torque box. Table 2.5 lists the Lockheed-specified wing planform parameters. Aluminum was used for all structural elements in the wing, with Al 2024 used on the bottom surfaces and Al 7075 used for the top surfaces, as is standard practice for aluminum wings.

Table 2.5: Wing Planform Geometry

Span	180.2 feet
C/4 Sweep	35.0 degree
Root chord	29.3 feet
Tip chord	8.8 feet
MAC	20.9
Area	3,425.8 sq feet
AR	9.5
X apex (leading edge junction)	44.9 feet
Y apex (leading edge junction)	0.0 feet
Z apex (leading edge junction)	19.6 feet
X C/4 MAC	44.7% fuselage length
t/c root	16.3%
t/c tip	11.6%

2.4.3 Determination of Structural Parameters

2.4.3.1 Reference Frame

Figure 2.9 is a schematic showing the positions of the structural elements which will be referred to throughout this section. The coordinate system used in this design places x in the axial direction with $x = 0$ representing the leading edge, y spanwise perpendicular to x with $y = 0$ representing the centerpoint in the span of the wing, and z in the vertical direction with $z = 0$ representing the bottom of the airfoil.

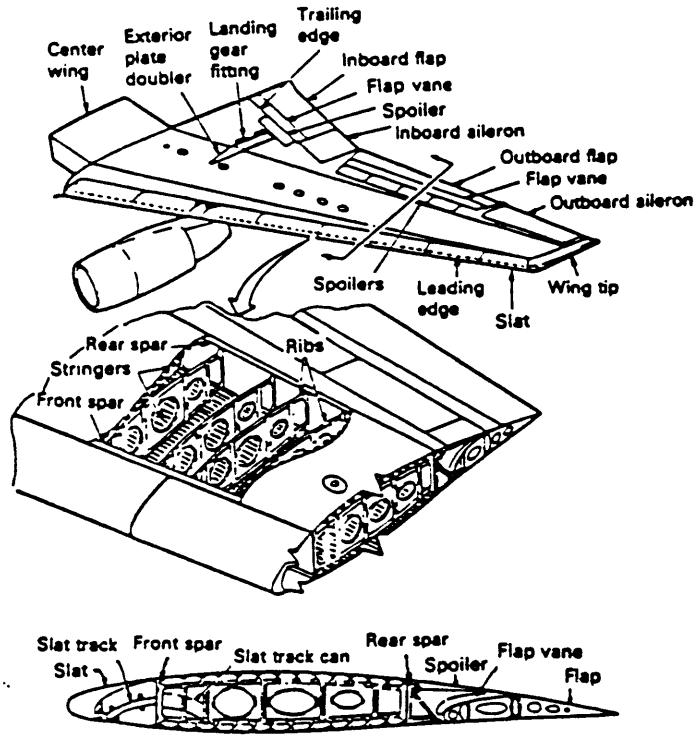

Figure 2.9: Structural Reference Frame (Ref. 8)

2.4.3.2 Calculation of Torsional Rigidity

The torque box includes the area between the forward and rear spars:

$$A_{bx} = h_f(x_{fs} - x_{rs})\, c \tag{2.1}$$

where A_{bx} is the area of the torque box, h_f is the height of the airfoil, x_{fs} represents the axial location of the front spar (distance of the front spar from the leading edge), x_{rs} the axial location of the rear spar, and c is the chord length at the particular spanwise location.

From this information, the torsional moment of inertia is given by:

$$J = \frac{4A^2}{\int \frac{1}{t} ds} = \frac{4A_{bx}^2}{\frac{c\,(x_{rs} - x_{fs})}{t_t} + \frac{c\,(x_{rs} - x_{fs})}{t_b}} \tag{2.2}$$

where t terms represents thicknesses of the top and bottom skin. Structural property equations used in this section can be found in Ref. 9.

The shear modulus, G, for Aluminum is 4.0 x 10^6 psi. Torsional rigidity is given by GJ.

2.4.3.3 Calculation of In-Plane Bending Stiffness

Airfoil height was determined geometrically from the baseline configuration. The airfoil height is given by

$$h_f = 0.09c\frac{\left(\frac{t}{c}\right)}{0.12} \tag{2.3}$$

t in this case represents airfoil thickness.

Next was the determination of respective areas for the top and bottom of the torque box. These areas are given by

$$A_{t,\,b} = n_{st}A_{st} + A_{fs} + A_{rs} + t_s\,(x_{rs} - x_{fs}) \tag{2.4}$$

where n_{st} is the number of stringers, A_{st} is the cross-sectional area of each stringer, A_{fs} is the cross-sectional area of the front spar cap, A_{rs} is the cross-sectional area of the rear spar car, t_s is the thickness of the skin in question (top and bottom), x_{rs} is the axial location of the rear spar, x_{fs} denotes the axial location of the front spar.

The z center of mass is given by

$$\bar{z} = \frac{A_t h_f}{(A_t + A_b)} \tag{2.5}$$

where z=0 denotes the bottom of the airfoil (as defined earlier).

In-plane moment of inertia is given by

$$I_{xx} = A_t\,(z_t - \bar{z})^2 + A_b\,(z_b - \bar{z})^2 = A_t\,(h_f - \bar{z})^2 + A_b\bar{z}^2 \tag{2.6}$$

The modulus of elasticity, E, is 1.05 x 10^7 psi. In-plane bending stiffness is given by EI_{xx}.

2.4.3.4 Calculation of Out-of-Plane Bending Stiffness

Out-of-plane inertia, I_{zz}, is given by the following relation:

$$I_{zz} = \iint (x - \bar{x})^2 dxdz \tag{2.7}$$

which is approximated by the discrete sum:

$$I_{zz} = \Sigma A x^2 - \Sigma A \bar{x}^2 \tag{2.8}$$

with the x-centroid given by:

$$\bar{x} = \frac{\Sigma A x}{\Sigma A} \tag{2.9}$$

This discrete approximation was used for the stringers and spar caps. Locations and areas of both the stringers and spar caps are known. For the case of the skin (continuous mass), an exact integral can be computed. This is given by:

$$\iint (x - \bar{x})^2 dx dz = \int_{x_{fs}}^{x_{rs}} (t_t + t_b)\ (x - \bar{x})^2 dx \tag{2.10}$$

where t_t and t_b denote the top and bottom skin thicknesses, respectively. This term is added to the summation for the discrete terms to produce overall I_{zz}. Multiplying by E yields the out-of plane bending stiffness, EI_{zz}.

2.4.3.5 Determination of Coupling Plane Bending Stiffness

This derivation is similar to that of EI_{zz}. The coupling inertia term, I_{xz}, is given by:

$$I_{xz} = -\iint (x - \bar{x})\ (z - \bar{z})\, dx dz = -\iint (xz - \bar{x}\bar{z})\, dx dz \tag{2.11}$$

with a discrete approximation given by:

$$I_{xz} = \Sigma A \bar{x} \bar{z} - \Sigma A x z \tag{2.12}$$

The center of masses, $\bar{x}$ and $\bar{z}$, were determined by the in-plane and out-of-plane stiffness derivations. For the discrete cases of the stringers and the spar caps, $\Sigma A x z$ can be determined because the locations of the elements are known. In the case of the skin, the appropriate integral is:

$$I_{xz} = -\int_{x_{fs}}^{x_{rs}} (x - \bar{x})\ (\,(z - \bar{z})_t t_t + (z - \bar{z})_b t_b)\, dx = -\int_{x_{fs}}^{x_{rs}} (x - \bar{x}) \left(\frac{h_f t_t}{2} - \frac{h_f t_b}{2} \right) dx \tag{2.13}$$

EI_{xz} is computed from this.

2.4.4 Mass Distribution

For the purposes of this design, the wing empty mass percentage breakdown was set to the following for the baseline case:

Leading Edge Mass = 5% of total

Trailing Edge Mass = 35% of total

Torque Box Mass = 60% of total

Overall torque box mass was reduced for the more flexible cases, while leading edge and trailing edge masses remained the same. Determination of torque box mass reductions is discussed in Chapter 4.

2.4.4.1 Determination of Leading Edge Mass

The leading edge mass per length for each spanwise location is proportional to chord length and is thus given by the following relation:

$$M_{le} = \frac{0.05cw_t}{A_{ws}} \tag{2.14}$$

where w_t is the total wing mass and A_{ws} is the wing surface area.

2.4.4.2 Determination of Trailing Edge Mass

Similarly, mass of the trailing edge per unit span is:

$$M_{te} = \frac{0.35cw_t}{A_{ws}} \tag{2.15}$$

2.4.4.3 Determination of Torque Box Mass

The torque box mass is assumed to be proportional to its EI, with B defined as the constant of proportionality.

$$m_b = BEI \tag{2.16}$$

Here EI is taken to be EI_{xx}, except that all structural elements in the torque box but the skin are neglected (an assumption that in this application yields a very accurate answer because of the relatively similar spanwise distribution of masses of all of the elements). EI and torque box mass, m_b, in this simplified model, are given by:

$$EI_{xx} = 2EA_s\left(\frac{h_f}{2}\right)^2 \tag{2.17}$$

$$m_b = g\rho_{Al}2A_s \tag{2.18}$$

where A_s is the area of the skin, h_f is the airfoil height, g is acceleration due to gravity, and ρ_{Al} is the density of aluminum.

Combining equations 2.16 and 2.17 yields:

$$n_b = 2g\rho_{Al}\frac{EI_{xx}}{2E}\left(\frac{2}{h_f}\right)^2 \tag{2.19}$$

or:

$$m_b = \frac{4g\rho_{Al}}{E}\left(\frac{1}{h_f}\right)^2 EI_{xx} \tag{2.20}$$

where g is the acceleration of gravity and ρ_{Al} is the density of aluminum.

Recalling the equation for h_f,

$$h_f = 0.09c\frac{\left(\frac{t}{c}\right)}{0.12}$$

The torque box mass equation can now be presented in terms of already available design parameters:

$$m_b = 4\left(\frac{0.12}{0.09}\right)^2\frac{g\rho_{Al}}{\left(\frac{t}{c}\right)^2 c^2 E}EI_{xx} \tag{2.21}$$

Equation 2.21 presents a useful relation for determining the effect of chord, thickness to chord ratio, and EI_{xx} on torque box mass. B therefore can be taken to be proportional to the term in front of EI_{xx} in equation 2.21. The constant multiplier of B is one which brings the torque box mass up to 60% of the empty wing weight. In this case, that multiplier is 2.92. So, B is given by:

$$B = 2.92 \cdot 4 \cdot \left(\frac{0.12}{0.09}\right)^2\frac{g\rho_{Al}}{\left(\frac{t}{c}\right)^2 c^2 E} \tag{2.22}$$

2.4.4.4 Determination of Fuel Mass Distribution

Overall fuel weight included in the wing is 114,931 pounds. Fuel mass per unit span M_f is given as follows:

$$M_f = ct\frac{w_f}{V_{tb}} = c^2\left(\frac{t}{c}\right)\frac{w_f}{V_{tb}} \tag{2.23}$$

where V_{tb} is the volume of the torque box, t is the thickness of the airfoil, w_f denotes fuel weight, and c represents the chord.

Fuel is placed out to 85% of the half span. Torque box volume in the equation represents the volume out to 85% of half span. It should also be noted that terms representing fuel weight in the equation are for half of the total fuel mass, because total fuel mass accounts for fuel placed in both halves of the wing.

2.4.4.5 Engine Mass

Each of the CF6-80C2 engines specified for this project weighs 15,000 pounds and will be attached with an engine pylon at 411 inches along the half span (Ref. 10). The offset between the engine center of mass and the pylon is -198.80 inches along the chord, -93.03 inches along the span, and -80.945 inches normal to the wing. The reader can refer to Figure 2.6 for a visual representation of engine placement. Engines act as point masses at their points of attachment.

2.4.5 Other Parameters

Center of gravity along the chord is calculated by assuming center of masses for each of the contributions to mass:

$$\frac{X_{cg}}{c} = 0.4M_f + 0.382BEI_{xx} + 0.075M_{le} + 0.0825M_{te} \tag{2.24}$$

Zero load values of x and z due to sweep and dihedral respectively were obtained from the baseline configuration geometry. Also specified by the baseline configuration are built-in twist, zero degree angle-of-attack, and the placement of the ailerons along with their effects on lift and moment per degree deflection.

2.5 Functional Analysis

2.5.1 Overview

The objective of functional design is to facilitate the design, definition, and development process. Functional analysis is a systematic approach for translating system technical requirements into specific qualitative and quantitative design requirements. Within the context of functional analysis is a tool known as a functional flow diagram. A functional flow diagram is a pictorial scheme used as a mechanism for portraying system functional requirements, illustrating series and parallel relationships, and establishing a hierarchy of system functions.

2.5.2 Functional Flow Diagram

For the purposes of this design, a functional flow was created in order to identify potential design variants. The top-level functional flow diagram is shown in Figure 2.10.

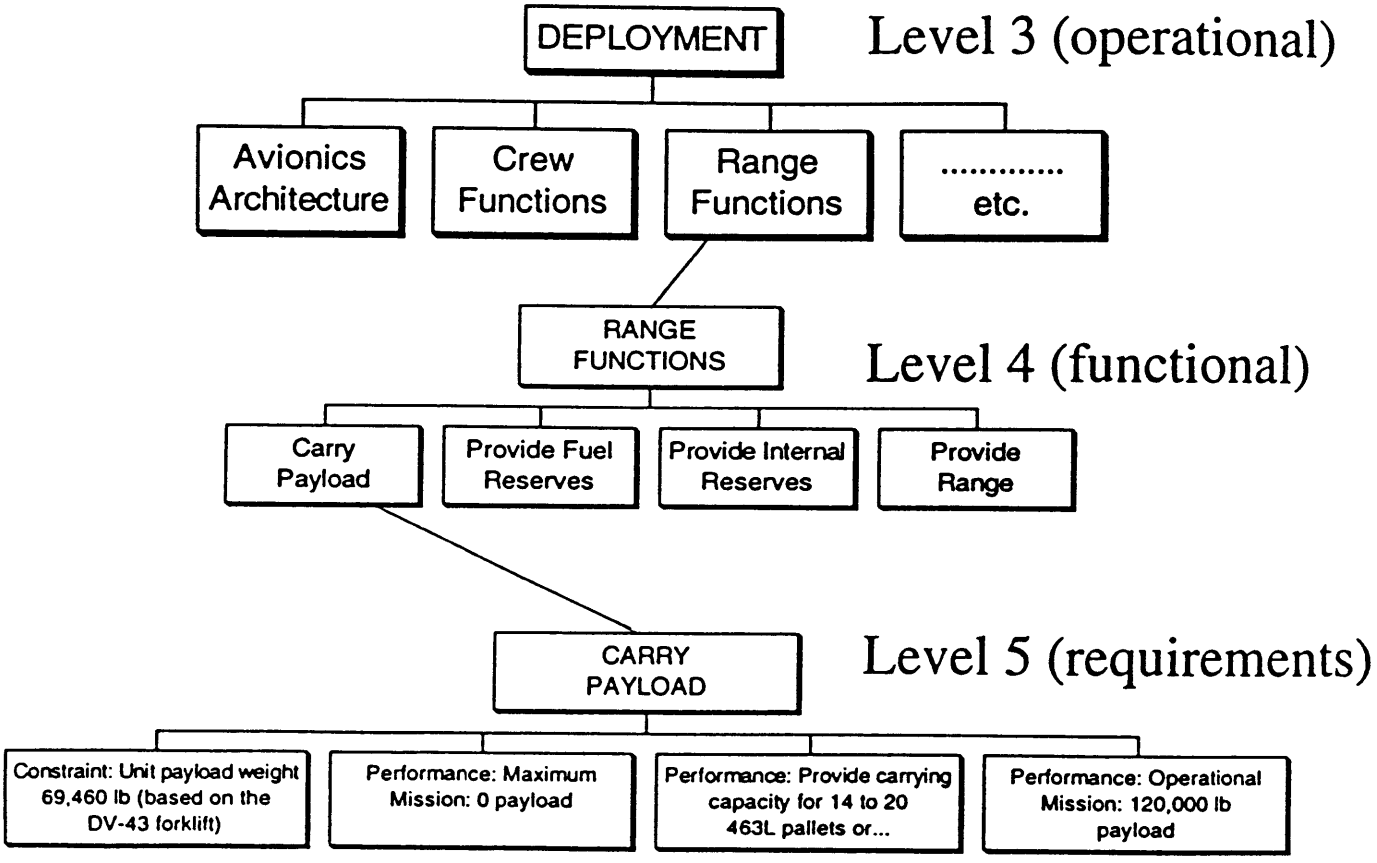

Figure 2.10: Top Level Functional Flow

2.5.3 Design Variants

The following possible design variants were identified:

- structural material for the wing can be either metal, composite, or a hybrid combination of the two
- size of control effectors can be changed and they can be placed at both the front and back of the wing planform
- conventional and AFW technologies could be mixed by changing the degree of wing flexibility
- the high-lift system can be broken up into multiple parts to accommodate bending

Because only one design iteration is used for this project, wing flexibility is the only design variant examined. The remainder are left for future AFW research.

2.6 Physical Design Questions

In order to better satisfy the functions and requirements of the NSA using AFW technology, a set of physical design questions was developed:

Wing Structural Weight

- What is the desired material selection: metals/composites? Can the tailorability of composites be beneficial in an AFW?
- What are the potential weight savings with an AFW for a high aspect ratio wing?
- What are the potential penalties for systems integration and complexity?

Aerodynamic Efficiency, Flight Controls, and High Lift

- How does use of an AFW affect load alleviation?
- Can control surface reversal be exploited?
- How does use of an AFW affect elastic mode control?
- How is high-lift integration affected by an AFW?

Reliability, Maintainability, and Supportability

- What are the reliability, maintainability, and supportability issues that may affect the implementation of AFW technology?

This project examines the issues of weight savings, aerodynamic efficiency, and controllability. Remaining issues are left for future study.

Chapter 3

Design Process and Computer Tools

3.1 Design Process Overview

Having determined requirements for the NSA, a design process was formulated to translate these requirements into a baseline wing design. Figure 3.1 shows a schematic of the wing design process used in this project. As discussed in Chapter 2, aircraft geometry was the starting point of the design process. From this, and from empirical data, a wing structural arrangement was determined. This wing structural arrangement along with planform and control surface layout was input into a computer tool known as ACAD (Advanced Computer Aided Design), chosen because of its excellent drawing and geometric analysis capabilities. ACAD produced the wing geometry used in this project. The program is also a preprocessor for ASTROS (Automated Structural Optimization System). ASTROS was chosen for use in the project because of its overall excellent interdisciplinary analysis of wings. ASTROS took as an input a finite element model determined from ACAD geometry. It then performed an air loads analysis, a sensitivity analysis, and a structural analysis. Structural analysis was performed using the finite element model and the determined loadings. Geometry from ACAD along with flight conditions was also input into ASWING, a multi-discipline design tool which uses lifting line theory to predict airloads and nonlinear beam theory to predict structural loads. Sizing of structural elements was input into ASWING from ASTROS. ASWING and ASTROS were also used to validate each other's structural and aerodynamic predictions. The capacity for ASWING to quickly incorporate changes in wing structure led to its being chosen for use in sensitivity analysis, while ASTROS was used to produce a high-fidelity model of the wing structural weight.

3.2 ACAD Description

ACAD is the primary computer tool used by Lockheed Fort Worth Company's Advanced Programs for configuration design of aircraft, both new and existing. The program was initially developed starting in 1982 by the Design Methods Group, a section

of Advanced Programs, with the main goal being to facilitate the preliminary design process by eliminating drawing boards and reducing design iteration time. The program's main role is the generation of geometry; however it does perform limited analysis. Wireframes, surfaces, and solids can be used to model geometry in both two and three dimensions. Geometry can then be downloaded into a postscript file, and hardcopy outputs can be obtained. A full description of ACAD is given by Ref. 11. For discussion of the use of ACAD in this project refer to Ref. 12.

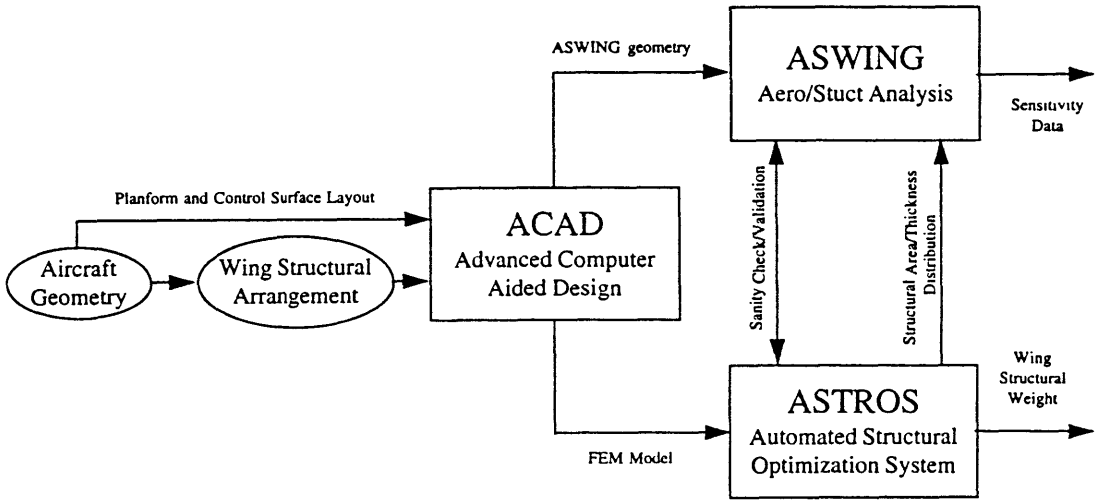

Figure 3.1: Wing Design Process Elements

3.3 ASTROS Description

ASTROS is a broad-based, multidisciplinary computer tool used for the analysis of wings and the interactions between structures, aerodynamics, and control systems within the wing. There are six major functions performed by ASTROS: design optimization, sensitivity analysis, structural analysis, air loads analysis, aeroelastic analysis, and control response. Design optimization is accomplished using the Automated Design Synthesis procedure. The program searches for the lowest weight design possible that satisfies specified structural and aerodynamic constraints. Sensitivity analysis involves the calculation of analytic derivatives for response methods in order to determine the effects of varying parameters and constraints. Structural response is determined by finite element

analysis, with response gauged in terms of stresses, strains, strain energies, natural frequencies, and displacements. Air loads analysis is performed based on a panelling method known as USSAERO-C, with minor modifications. Aero loads are coupled with structural loads. Aeroelastic analysis is based on flutter calculations. ASTROS also analyzes the interactions between a control system and the wing structure in order to determine structural response and control effectiveness. A full description of ASTROS is given by Ref. 13. For discussion of the use of ASTROS in this project, refer to Ref. 12.

3.4 ASWING Description

ASWING was developed by Mark Drela at MIT as a tool to perform structural and aerodynamic analysis of flexible high-aspect ratio wings. Initially, the program was used for modelling of the small human-powered plane Daedalus, but was modified to account for arbitrary sweep angle to allow for use on the wings in this project. Nonlinear beam theory is used for the structural model, with up-down, fore-aft, and torsional deflections allowed. No limit is placed on the magnitude of these deflections. Prandtl lifting-line theory is used for the aerodynamic model, applied to the deflected wing geometry. Hence, the structural and aerodynamic models are fully coupled. A complete description is included in Ref. 14.

3.5 ASWING Input File

In order to determine the values of variables in the input file, a MATLAB script was written which computed the necessary structural and aerodynamic parameters from structural element sizing and the assumed wing planform. This input file is located in Appendix C. Structural element sizing for the ASWING build was based primarily on ASTROS results. In the ASWING case, unlike ASTROS, the sizing distribution is assumed to be linear from root to tip. Structural parameters were calculated at spanwise locations corresponding to termination of stringers, flaps, engine pylons, and the end of the fuel tank.

3.6 Sensitivity Analysis Using ASWING

Parameters considered in the sensitivity analysis were ratio of torque box mass to that of the baseline wing torque box mass (baseline wing torque box mass given by ASTROS sizings and used in the ASWING input file), tip washin angle, and flight load factor. These parameters were analyzed to determine effects on spanwise efficiency, aileron reversal speed, maximum spanwise strain, and maximum spanwise shear. The parameters specified in Table 3.1 were kept constant throughout the analysis.

Table 3.1: Constant Flight Conditions in ASWING Analysis

Flight Conditions
Gross weight = 380,000 lbs
Altitude = 32,000 ft.
Flight Mach number = 0.82

ASWING allows for direct linear scaling of any or all input file parameters, with the values affected at all spanwise locations. This feature was used in the analysis as the torque box weight was altered. As described earlier, the weight of the torque box is assumed to scale directly with all of the bending stiffnesses and torsional rigidity.

3.7 Risk Management

Because an AFW had never before been examined using any of these programs, the project was structured to avoid dependency on any one of these codes alone. ACAD geometry was not affected by the AFW alterations, because it was only used for drawing the baseline configuration. If the program had failed, Lockheed-provided planform parameters and a sketch of the baseline wing would have been used for estimates of the wing geometry that would have been input into ASTROS and ASWING. The sensitivity analysis of ASWING could have been performed by ASTROS, although it would have been a much more time-consuming endeavor. Similarly, if ASTROS had not been able to output structural data, a spreadsheet analysis would have been used for the task, although with much less fidelity.

Chapter 4

Results

4.1 Overview

As specified in Chapter 3, both the baseline wing and the flexible wing variants were analyzed using computer codes ASTROS and ASWING. ASTROS provided sizing of structural components and deflections under design-intended flight conditions. ASWING was used to "fly" the airplane through different points on the V-n diagram and determine deflections, stresses, strains, reversal speeds and span efficiency. Because of the versatility of ASWING, the program was used to perform comparisons between the baseline and more flexible wings, as well as to determine the effect of washin on the wing.

4.2 Wing Sizing Results

Inputs into ASTROS were the NSA baseline configuration provided by Lockheed, the structural layout as specified in Chapter 2, and the V-n diagram for the intended military deployment mission. ASTROS produced sizing distributions of structural elements along the span, as well as deflections under the loading conditions encountered during the mission. These sizings were incorporated into the baseline wing. For the baseline wing, a conservative yield criteria was used for sizing, such that the wing could be made more flexible. The effects of increased flexibility were examined in the sensitivity analysis. Stringers were not included in the ASTROS model, but are included in the ASWING analysis. This difference was due to the complexity of entering stringers into ASTROS. Table 4.1 shows the root and tip sizings of structural elements for the ASWING build. A more complete discussion of the use of ASTROS in this project as well as the elemental sizing results throughout the span can be found in Ref. 12.

4.3 ASWING validation of ASTROS deflection results

ASWING computed results for several flight conditions, and wing deflections were compared with those determined by ASTROS for the same conditions. The results compared favorably. To quantify this result, for Mach 0.69, equivalent airspeed 239 knots,

and 2.5 g of loading, ASTROS tip deflection was 16.9 feet and ASWING tip deflection was 17.6 feet, a difference of less than 5%.

Table 4.1: ASWING Structural Element Sizing

Structural Element	Root	Tip
Top forward spar (in^2)	16.0	0.5
Top aft spar (in^2)	15.0	0.5
Bottom forward spar (in^2)	17.0	0.5
Bottom aft spar (in^2)	50.0	0.5
Top skin thickness (in)	0.50	0.05
Bottom skin thickness (in)	0.50	0.05
Stringers on top (in^2)	1.06	0.53
Stringers on bottom (in^2)	0.86	0.43

4.4 Effect of Flexibility on Wing Weight

For the purposes of this study, a parameter K was created and defined to be the ratio of the torque box weight of the wing in question to the torque box weight of the baseline wing. Thus, $K = 1$ for the baseline wing. Change of overall structural weight due to change in K, denoted by ΔK, is given by:

$$\frac{\Delta W}{W_0} = \left(\frac{w_{bx}}{w_{le} + w_{te} + w_{bx}} \right) \Delta K = 0.60 \Delta K \tag{4.1}$$

where W is the wing structural weight, the w terms represent respective weights listed as follows: w_{le} is the leading edge weight, w_{te} stands for the trailing edge weight, w_{bx} is the weight of the torque box of the baseline wing. It should be noted again that the above equation represents a simplification used here solely to illustrate trends. If a full wing with $K < 1$ was designed, the actual wing structural weight would be determined by an iterative process, and would be lower than that given by equation 4.1.

4.5 Aileron Control Effectiveness

Roll rates for 1-g maneuvers were examined as a function of equivalent airspeed for both the baseline torque box K=1 and a torque box that was reduced to 60% (K=0.60) of its original mass (24% lower wing structural weight). Factoring in the wing structural weight to the weight of the aircraft, the K = 0.60 torque box leads to a 3.2% uniterated gross takeoff weight as compared to the baseline torque box case. Uniterated weight means that no further design cycles were performed to scale down the entire configuration in response to this component weight reduction. In actuality, gross takeoff weight savings would be greater. Figure 4.1 is a graph of roll rates for the two cases versus flight velocity with a five degree aileron deflection.

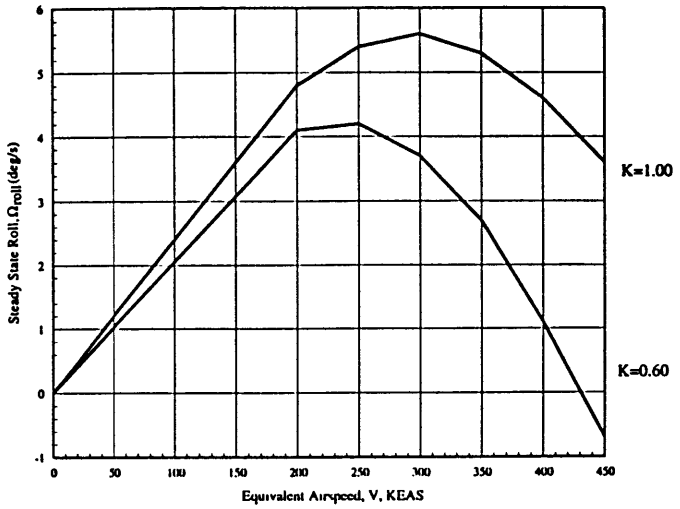

Figure 4.1: Aileron Control Effectiveness

For a completely rigid wing, steady state roll rate is a linearly increasing function of airspeed. Flexibility has a continually greater effect in reducing aileron effectiveness as dynamic pressure is increased.

Control effectiveness can be quantified by the parameter $\frac{\Omega_f}{\Omega_r}$,.which is the roll rate for an aileron deflection relative to what it would be for a rigid wing. From Figure 4.1, one can see the drop-off in control effectiveness from a rigid wing as compared to a flexible wing. A lower value of $\frac{\Omega_f}{\Omega_r}$ means that either a larger aileron deflection or a bigger aileron surface is required to produce the design roll rate. There is a physical limit to aileron deflection and sizing, which could place a restriction on use of conventional controls on flexible wings. A more in-depth analysis, which would examine structural effects of large

aileron deflections and sizings, would be needed to determine whether this reduction in control effectiveness is a significant design problem. If desired roll rate could not be achieved by a flexible wing, a conventional high speed inboard aileron (see Figure 2.10) could be designed that would be used when the outboard aileron loses effectiveness. It should also be noted that for both torque box masses, the value of $\frac{\Omega_f}{\Omega_r}$ is equal to approximately 0.70 at the point where roll rate begins to drop.

Reversal speed (the velocity at which roll rate is zero) decreases with increasing wing flexibility (about 25% lower for K = 0.60 as compared to K = 1. As can be seen from Figure 4.1, reversal velocity occurs at 430 knots equivalent airspeed (KEAS) for the reduced weight torque box case. Therefore, the issue of aileron reversal is not a factor for this design, and conventional control surfaces can be used. Production of a design which would include reversal phenomena would likely involve having more than two spars and/ or different material selection (Ref. 15).

4.6 Maximum Strain

Maximum strain (highest value of strain at any spanwise location) is important structurally in a wing design because often a wing is sized by its yield point, meaning structure is designed such that at worst expected case scenarios for dynamic pressure during flight, the wing would be on the verge of yielding. Figure 4.2 shows the predicted effect of washin angle t and stiffness (torque box mass) on maximum strain:

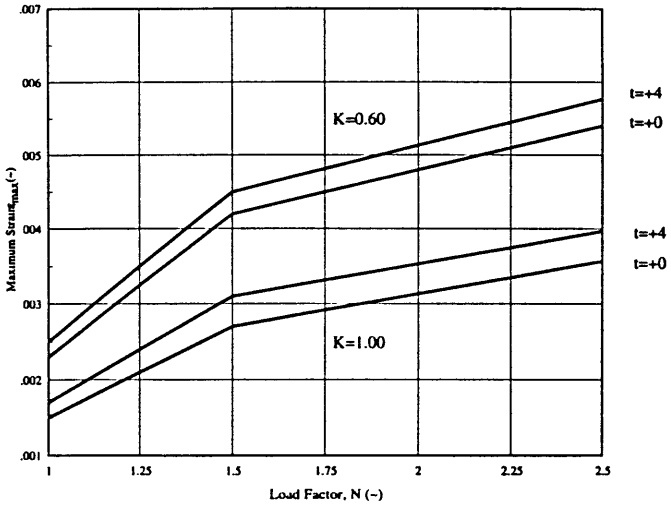

Figure 4.2: Maximum Strain

Stiffness, as expected, has a significant effect on maximum strain. This is because bending and torsional stiffness parameters, EI and GJ respectively, are strong drivers of strain calculations. In this case, a 40% reduction in torque box weight leads to about a 45% increase in strain, with the percentage increase being approximately the same over several load factors. Washin angle, on the other hand, has an effect of only about 6.5% effect on strain for the 4 degree change that is examined here. In the reduced torque box case, the value of maximum strain approaches 0.006 (aluminum's yield value) as the design load of 2.5 g is approached. This does not imply that the torque box weight could not be reduced any further because different sizing distributions of structural elements would yield different strain results. However, the sharp increase in strain due to flexibility represents an important factor in a flexible design. One possible result of this is that stiffer materials will tend to be chosen for flexible wings.

4.7 Maximum Shear Stress

As with strain, shear stress was calculated as a function of washin angle t and torque box stiffness. Results are summarized in Figure 4.3.

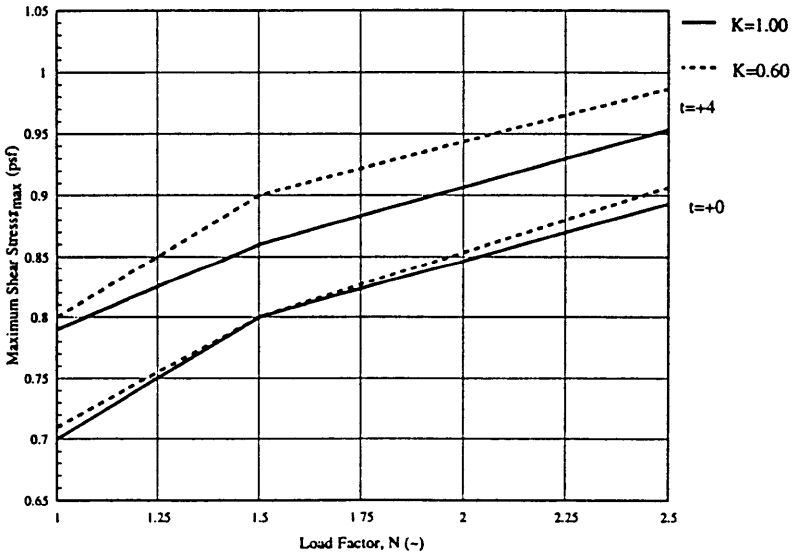

Figure 4.3: Maximum Shear Stress

In the shear stress case, it is not stiffness but rather washin angle which has the strongest influence, causing a dramatic increase in shear stress. This is due to the effect of washin in moving the centroid of the half span lift further outboard, thereby creating a

more elliptical lift curve distribution. Figure 4.4 shows lift distributions along the K = 1 wing at cruise without washin and with 4 degrees of washin. The dotted line represents no washin, whereas the solid line represents a washin of 4 degrees.

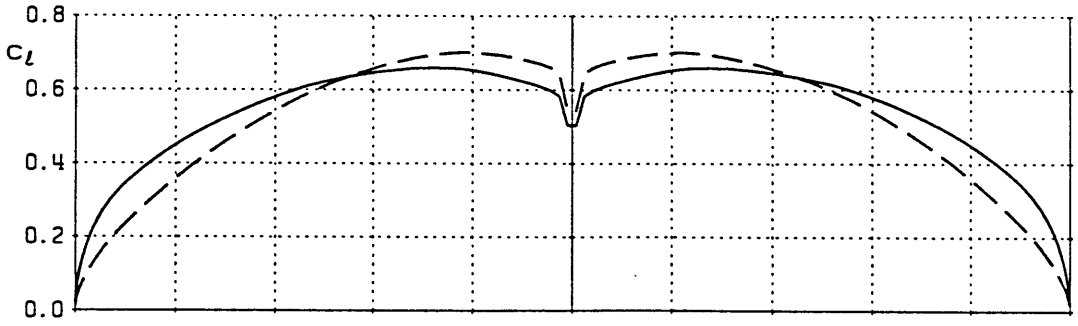

Figure 4.4: Lift Distributions with and without washin

Although the absolute values of shear stress indicated in this analysis do not reach the structural limiting value for aluminum, the trend of increased shear with washin angle is important because it may place a limit on the amount of washin angle in a design.

4.8 Span Efficiency

For the purposes of this analysis, span efficiency e is taken to be

$$\frac{S_o}{\pi b_o^2}\frac{C_L^2}{C_{Di}} = e \tag{4.2}$$

where b_0 represents the zero-load span, S_o the zero-load wing surface area, C_L^2 is the square of the lift coefficient, C_{Di} is induced drag. The zero-load span is used so that e is strictly a measure of C_{Di} relative to C_L^2. If the loaded span was used instead of b_o, the interpretation of e would be less clear. Figure 4.5 shows the effect of weight reduction and washin angle on span efficiency. Three points were analyzed: K = 1, 0.80, 0.60.

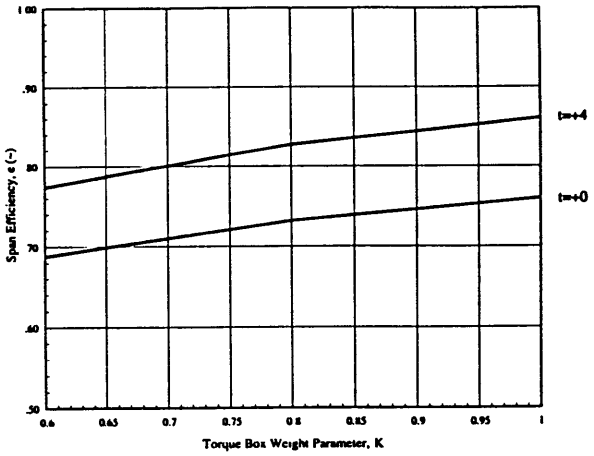

Figure 4.5: Span Efficiency vs. wing weight, washin angle

Without factoring in washin angle, the wing with reduced torque box weight had about an 11% decrease in span efficiency over the baseline one. Physically, this makes sense because the flexibility associated with reduced torque box weight produces deflections which decrease lift at the tips; the resultant load distribution is quite far from elliptical (the optimum aerodynamic distribution). Load plots for the cases (K=1 and K=0.60) are shown by Figure 4.6 and 4.7 respectively. Again, the dotted lines represent no washin; solid lines are 4 degrees washin.

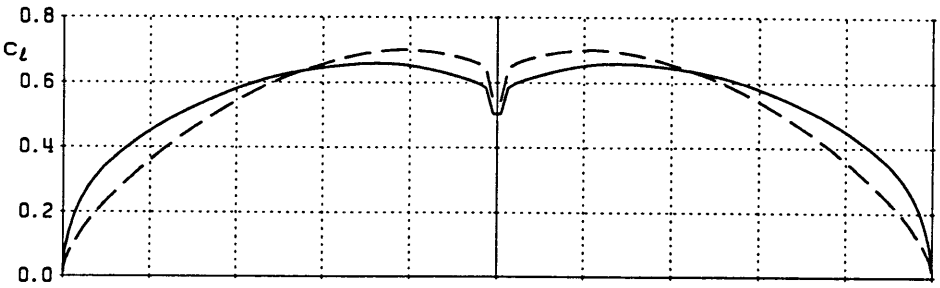

Figure 4.6: Load distribution on K=1.0 torque box

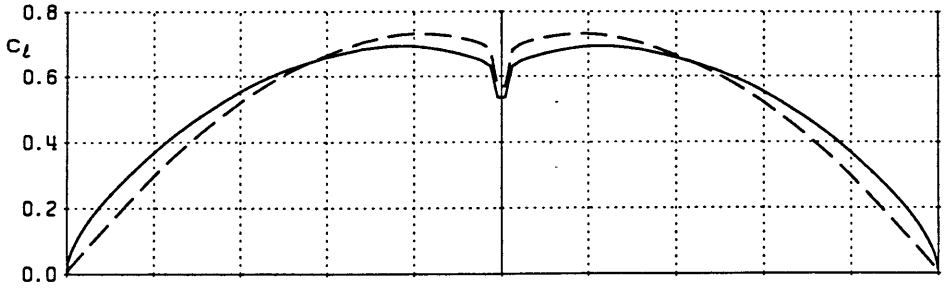

Figure 4.7: Load distribution on K=0.6 torque box

Increasing the washin angle from 0 to 4 degrees has the effect of increasing span efficiency by about 12%. This is a direct result of increased washin pushing the load further outboard, and thus creating a more elliptical, and hence a more efficient, load distribution. Adding more washin with reductions in K is clearly important to maintain span efficiency. The present sensitivity analysis indicates that approximately 0.8 degrees of washin are needed for a 0.1 reduction in K. However, as noted earlier, increasing the washin angle has a dramatic effect on increasing shear stress. Thus, in a flexible wing design, there may be a limit on washin angle and hence span efficiency may be lower.

4.9 Overall Effect of Flexibility in Wing Design

Table 4.2 shows a comparison of the properties of the flexible wing design in the K = 0.60 case and the baseline K = 1.0 wing.

Table 4.2: Comparison of Flexible and Baseline Wings

Property	Flexible Wing	Baseline Wing
Torque Box Weight Reduction	40%	0%
Roll Rate at Cruise (aileron deflection = 2 degrees)	2.38 degrees	5.22 degrees
Reversal Speed	430 KEAS	> 700 KEAS
Maximum Strain (no washin)	0.0023	0.0015
Maximum Strain (with washin)	0.0025	0.0018
Maximum Shear Stress (no washin)	0.91 psf	0.89 psf
Maximum Shear Stress (with washin)	0.98 psf	0.95 psf
Span Efficiency (no washin)	0.69	0.76
Span Efficiency (with washin)	0.77	0.86
Failure Speed	380 KEAS	> 600 KEAS

The most significant result of this study is that for this particular wing configuration and structural layout, reversal speed is not reached within the flight envelope, unlike the fighter wing case (Ref.1). Thus, conventional control surfaces would be used in the flexible wing design, although such control surfaces either might be larger than those used

in the baseline wing or there might be a different scheduling of a conventional high-speed aileron. For this particular design, the potential advantages that are foreseen by the use of AFW control mechanisms, such as tailored aero efficiency, increased aerodynamic performance at off-design points and full wing-tip generated roll control power are not available.

Significant structural weight savings was realized by increasing flexibility. Because of the importance of aircraft cost for this design (highest priority in the QFD of Chapter 2), the weight savings represents a very important benefit of flexible wing technology. Considering the subset of important design parameters that was examined in this study, a total wing structural weight savings of 24% for the flexible wing was obtained before the wing reached its structural limits. It is important to note here that not all important design parameters were considered, and the possibility exists that a parameter not examined such as flutter could limit the weight reduction in the flexible wing. Assuming all other weights are constant in the plane, use of the flexible wing leads to an uniterated gross takeoff weight reduction of 3.2%. This weight savings will multiply at least severalfold in the actual, iterated gross takeoff weight, especially for long-range missions which benefit the most from reductions in empty weight (Ref. 15).

Increasing built-in washin angle is needed to maintain span efficiency in the flexible wing design. Washin angle must be increased with caution, however, because doing so tends to increase shear stress. If a certain span efficiency is specified, a limit of flexibility is reached when the washin angle needed to maintain span efficiency causes the structure to reach its maximum design shear stress value.

As expected, the flexible wing has a larger amount of strain throughout the span than the baseline wing. The increase in strain is roughly inversely proportional to torque box weight. In this particular case, strain limitations prohibit reduction of torque box mass for the flexible wing below 60% of the baseline wing. Thus, stiffer materials might be better suited for use on flexible wings.

Chapter 5

Project Conclusions

5.1 Project Contribution

To the author's knowledge, this project represents the first design investigation for AFW technology applied to a large transport aircraft. Contemporary requirements analysis techniques were used to identify important aspects of design of the proposed New Strategic Airlifter. The process of analyzing requirements yielded potential design variants and raised physical design questions pertaining to the use of AFW technology for transport applications. Issues of weight savings, aerodynamic efficiency, and control effectiveness were examined, yielding key relations for the implementation of AFW technology. Recommendations were made as to the design of flexible wings based on these relations.

5.2 Impact of Flexibility on Wing

As determined by the design studies performed during this project, significant weight savings were obtained by reducing the stiffness of a baseline wing. A flexible wing was designed by reducing the wing's stiffness to a point where the material was on the verge of yield. Considering the subset of parameters used in the study (stresses and strains), this is the limiting factor in the wing design. The 3.2% reduction in uniterated gross takeoff weight resulting from 40% torque box weight reduction as found in Chapter 4 can lead to a severalfold reduction in actual gross takeoff weight when all factors are considered.

Reversal speed is not reached in this design, and thus conventional control surfaces can be used. However these control surfaces must either be larger, deflect more than the baseline case, or be moved further inboard. Span efficiency is also reduced as flexibility increases, when only torque box weight is varied in the design. Washin is presented as a possible solution to this problem, but washin can only help to a certain extent as it has the effect of increasing shear stress in the wing.

5.3 Future Design Issues

Further research on the subject of AFW is strongly recommended. The flexible wing design in this project was feasible given the strain, shear stress, and span efficiency criteria that were examined. Future projects should examine effects on flexible wings of parameters that were not examined here. For example, what is the effect of flexibility on the flutter boundary. Also, a more in-depth study of the wing used in this project would consider thousands of points in the flight envelope, rather than just one.

Within the limited time allotted for this project, many potential variants on the design could not be examined. Most important is a design that would allow for control surface reversal to occur within the flight envelope. Such a design would allow for the theorized aerodynamic benefits of AFW technology, such as tailored aero efficiency increments, reductions in control surface size, and wing-generated roll power, to be examined. The inclusion of reversal phenomena in a design would likely mean that more than two spars would be used.

While the sensitivity analyses of this project yielded important trends, future research should be done which incorporates the knowledge gained from these trends into a design. For example, it was suggested in Chapter 4, that stiffer materials and greater washin be used for the flexible wing design because of importance of strain and span efficiency respectively. It should be noted that these changes are complementary; stiffer materials require less washin to maintain span efficiency. A suggested project is one in which a stiffer material with greater designed washin is used from the beginning to identify new issues and produce a more feasible flexible wing. Successive iterations of such projects could lead to a viable flexible wing design which could replace conventional wings in some facets of the aerospace marketplace.

In addition, examination of flexible wing effects should consider system integration and reliability, maintainability, and supportability issues. Use of a flexible wing may significantly impact these issues. Of special note is the impact a flexible wing would have on the high-lift system, which may need to be broken up into multiple parts to account for bending near the root. Studies should be performed which identify potential "show stoppers," flexible wing effects which would severely cripple its ability to be implemented.

Appendix A

Project Logistics

A.1 Team Logistics

A two person design team consisting of the author and fellow student Jerry Wohletz carried out this project over a 4 1/2 month span. The project represents MIT's first Master of Engineering design project. Lockheed was the primary corporate sponsor of the project. The company provided computer tools, points of contact, and the baseline configuration of the New Strategic Airlifter. The following is a list of organizations and individuals involved in the project and their points of contact.

Lockheed Martin Aeronautical System Company

Luis Miranda	Flight Sciences
Mark Norris	Advanced Design
Steve Justice	Advanced Design
Charlie Griffin	Advanced Structural Design

Rockwell International - North American Aircraft

Gerry Miller	Advanced Structural Design

NASA - Langley

Boyd Perry	Aeroelasticity Branch

Parker Bertea Aerospace

C. Ed Stevens	Actuator Design, Manager-Engineering Section

MOOG

Pete Neal	Principal Engineer- Controls

Wright Laboratories

Edward Pendleton	Advanced Aeroelastic Wing Program
Gerald Andersen	Advanced Aeroelastic Wing Program

A.2 Intended Project Schedule

The schedule laid out for the project by the requirements review is shown in Figure A.1. Although some of the items listed were never accomplished, this schedule lists the most important aspects of the design as determined by the requirements review process.

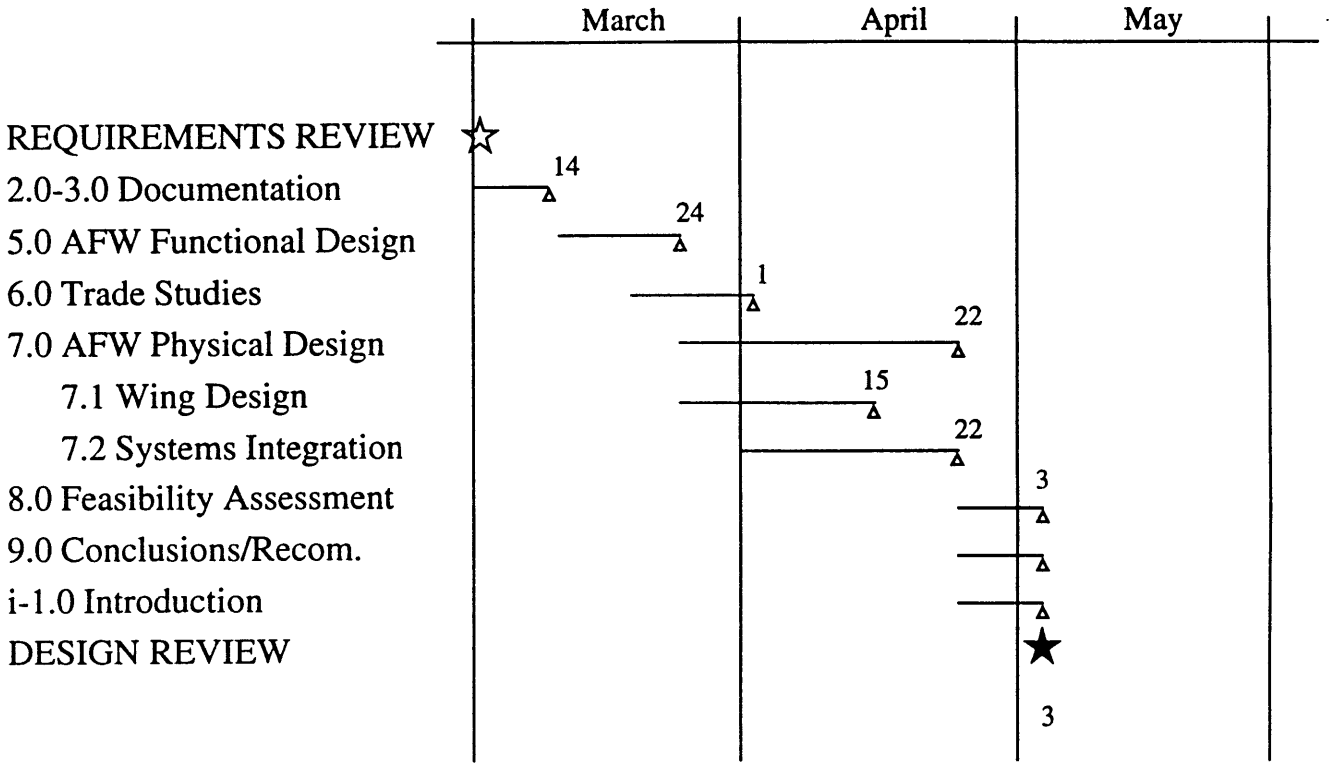

Figure A.1: Intended Project Schedule

A.3 DeMAID Analysis of Design Process

Figure A.2 shows an analysis of design process steps by the computer program DeMAID (Design Manager's Aid for Intelligent Decomposition). DeMAID is an analysis program which takes needed functions in a design process, along with their interdependencies, and suggests an efficient sequence that they be performed in.

1 Read and interpret source material
2 Identify DOC design drivers
3 Create requirements hierarchy
4 Perform literature search
5 Create QFD build
6 Perform functional flow analysis
7 Identify design variants
8 Determine type and placement of controls
9 Perform trade studies
10 Determine loading of AFW
11 Determine structural arrangement of AFW
12 Integration of systems
13 Perform technology asessment
14 Perform risk assessment
15 Write conclusions and make recommendations

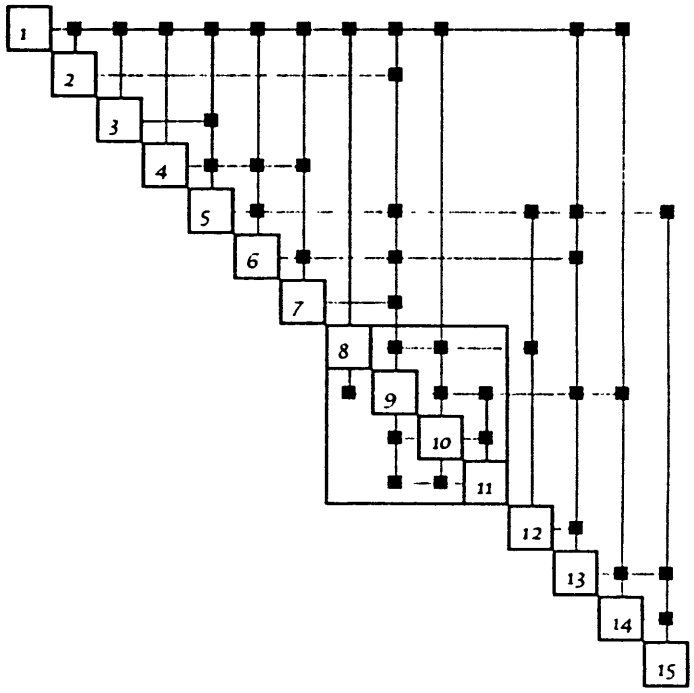

Figure A.2: DeMAID Output

Appendix B

Operational Requirements Document for Lockheed's New Strategic Airlifter

OPERATIONAL REQUIREMENTS DOCUMENT

New Strategic Airlifter

1. GENERAL DESCRIPTION OF OPERATIONAL CAPABILITY:

A. Mission Area:

Provide a new strategic airlifter (NSA) which fills the void created by the retirement of the C-141 fleet. US military strategy is increasingly dependent upon strategic airlift as forces are withdrawn from forward positioning and a central reserve is maintained within the US to be deployed in time of crisis. Mobility/transport aircraft will continue to play an important role in the future from large-scale conventional war to humanitarian aid and peacekeeping efforts. The new airlifter will also have airdrop and tanker capabilities. Additionally, commercial air cargo transport growth will outpace passenger growth for the foreseeable future. The new airlifter will therefore have commercial business applications ranging from overnight package services to high priority oversize shipping.

B. Type of Proposed System:

(1) This requirement can be broken down into two main markets:

1. Military (USAF / European Union / Rest of World)
    - Deployment
    - Airdrop
    - Tanker

2. Commercial (Domestic / International)
    - Overnight
    - Intermodal

(2) This ORD will concentrate on the "primary" military market. The aircraft design will be based on deployment since it possesses the dominate requirement parameters. The specific requirements for commercial and other operations will be outlined in Table 1.

C. Anticipated Operational and Support Concepts:

The NSA shall be FAA-certified. It shall have roll-on/roll-off capability and carry palletized bulk and oversize cargo. It will meet minimum Army requirements for personnel, containerized delivery system (CDS), and low velocity airdrop (LVAD) operations. Previously developed manuals (operations, maintenance, and performance) will be used to meet military requirements and restrictions.

2. THREAT:

The NSA will routinely operate in the same threat environment currently experienced by the C-141, C-5, and C-17 (in its non-tactical role).

3. SHORTCOMINGS OF EXISTING SYSTEMS.

The early retirement of the C-141 fleet combined with a possible reduction in C-17 procurement creates a shortfall in airlift capability. The shortfall could be alleviated to some extent with a NDAA procurement, however, the million ton mile per day requirements will still not be satisfied. Force delivery times required to meet strategic and tactical objectives could be jeopardized. There will also be a shortage in available tankers due to the aging KC-135 aircraft fleet which constitutes 82% of the tanker fleet. Additionally, the aging fleet of DC-8/707 freighters combined with the continued expansion in commercial air cargo requirements will create a gap that must be filled.

4. CAPABILITIES REQUIRED: (USAF Military)

A. **Basic Performance.** Operate in the organized track systems, comply with minimum navigation performance standards for worldwide operations, meet reduced vertical separation minima (RVSM) requirements, and be transoceanic capable. Flight performance must be compatible with commercial aircraft. Must meet FAA Stage 3 noise and ICAO pollution standards.

B. **Range/Payload.** Fly 3300 NM unrefueled, no wind, from a point of departure to first point of intended landing, with a 120,000 US pound payload and arrive with enough reserve fuel to go an additional 500 NM (per MACR 55-2). The maximum range will be 6000 NM with zero payload. The unit payload weight is 69,460 lb (based on the DV-43 forklift). The maximum dimensions per unit are height - 149 in (crane), width - 149 in (CH-47C helicopter), and length - 609 in (CH-47C helicopter). The aircraft should be able to carry 14 to 20 463L pallets or up to 200 troops.

C. **Minimum Runway/Turning.** Take off under the above range/payload conditions from a 7500 x 86 foot, level, dry, paved runway, standard day, at sea level with no obstacle, using USAF performance criteria. Required landing length under the same conditions is 5000 feet. Aircraft LCN $\geq$ 60. Turn requirements are 180 degrees on a 90 foot wide taxiway.

D. **Cruise Speed/Altitude.** Initial cruise altitude is 32,000 feet at a speed of .82 Mach. Max cruise altitude is 39,000 feet. Max cruise air speed of 350 KEAS or 0.86 Mach.

E. **Crew.** Flight crew requires 2 pilots and cargo crew requires 1 loadmaster. Up to 6 flight crew required for relief.

F. **Weight and Balance Information.** Onboard automated weight and balance computation system required. Integration with the flight management system (FMS) is desired.

G. **Mission Planning.** Automated capability to do aircraft performance analysis such as takeoff and landing data (TOLD), airfield analysis, flight planning, and essential information contained in DD Form 365-4 computation is required. This capability integrated with the FMS is desired.

H. **Flight Station.** Crew positions must be kept to a minimum. The desired objective is a two-pilot cockpit. A station for a loadmaster must be provided with oxygen/radio/interphone capability. An FMS is desired. System redundancy should be optimized to allow safe operation of the aircraft from pilot or copilot crew positions. The cockpit shall contain required emergency/survival equipment and devices to accommodate all crew positions.

I. **Cargo Capability.** Must carry palletized bulk and oversize cargo. Must be roll-on, roll-off rolling stock capable. The cargo floor height is 60 to 70 in above ground. Must have a 463L-compatible powered roller loading system and a 12 degree max ramp angle. Crew door dimensions are forward port 32 x 48 in.

J. **Reliability/Maintainability.** Design life of 45,000 flight hours with a maintenance man-hour per flight hour of 12.0.

K. **Environmental Conditions.** Operate from military and civilian airports worldwide and in all climatic conditions. The equipment shall be protected from and/or resistant to the effects of sand, dust, snow, ice, turbulence, salt-laden air, moisture, and temperature extremes. Aircraft must be able to operate in moderate icing conditions and be tolerant of moderate turbulence conditions. it must be capable of operating in instrument meteorological conditions (IMC) during day and night. Instrument flight rules (IFR)

capability is required to include Category (CAT) II instrument landing system (ILS) approaches. The aircraft must allow the crew to don chemical suits while in flight, land the aircraft, and egress safely.

L. **Propulsion.** Self-contained start capability. Aircraft operation shall accommodate a safe and routine capability of totally self-contained mission preparation/launch activity including shutdown and engine start from any operating location. Must be able to start with a ground and air power cart and have engine cross starting capability.

M. **Fuel System.** Control and monitoring should be a "set and forget" system with warnings. Failures should default to a fail-safe, flexible fuel sourcing backup mode. The aircraft/fuel system shall be compatible with JP-8 as the primary fuel and JP-4, -5 and commercial grades of Jet A, A-I, and B as alternate fuels. The system should be serviceable through a single-point receptacle, pressure/closed circuit refuel, and alternate gravity-feed refueling points to completely fill all tanks. Aerial refueling receiver capability is required.

N. **Airdrop Operations.** The airdrop of heavy equipment, personnel, or CDS will be used to secure key ground objectives or resupply friendly forces. Delivery airspeeds will be 130-135 KIAS for personnel, 150 KIAS for equipment/CDS and 130-150 KIAS for the door bundle. Minimum delivery altitudes will be 500-800 ft. for personnel, 600 ft. for CDS, 1000 ft. for heavy equipment and 300 ft. for the door bundle.

O. **Avionics Architecture.** The avionics system shall be certified for overwater operation in accordance with all military and civil qualifications. An avionics architecture providing an integrated solution for the following functions is desired: control and display of pilot/flight information, communications, navigation/identification, autopilot/flight director, and integrated diagnostics. The integrated avionics should employ state-of-the-art technologies to the max extent possible including such things as electronic color displays, graphics processor, and BIT. External interfaces should be provided between the avionics and other subsystems for integrating control/displays and diagnostics.

P. **Communications.** All crewmembers shall have the capability of transmitting and receiving on all command radios.

Q. **Survivability.** Make maximum use of current infrared (IR) technologies to minimize the proliferated IR missile threat. Shall be equipped with a standard airlift defensive system.

NEW STRATEGIC AIRLIFTER

	MILITARY (USAF / EUROPEAN UNION / REST OF WORLD)			COMMERCIAL (DOMESTIC / INTERNATIONAL)	
	DEPLOYMENT	AIRDROP	TANKER	OVERNIGHT	INTERMODAL
DESIGN PAYLOAD (TOTAL) KLBS	120	90 EQUIP,56.7 PERS.	180 FUEL OFFLOAD	82-140	82-140
DESIGN PAYLOAD (ITEM) KLBS	69.46	60	30	15	45
MAX HEIGHT (ITEM) IN	149	126	96	96	96
MAX WIDTH (ITEM) IN	149		125	96	96
MAX LENGTH (ITEM) IN	609		120	125	480
PALLETS	14-20 463L		2 M1 CONTAINERS	18-24	18-24
PASSENGERS	200 TROOPS	150-162 PARATR			
RANGE AT DESIGN PAYLOAD NM	3300 + 500	? + 500	1500 RADIUS	1800-3200	1800-3200
MAX RANGE NM	6000	6000	6000 MIN	6000 MIN	6000 MIN
INITIAL CRUISE ALT FT/MACH	32,000/0.82	32,000/0.82	32,000/0.82	32,000/0 80	32,000/0.80
MAX CRUISE ALTITUDE FT	39,000	39,000	39,000	39,000	39,000
Vc KEAS/Mc	350/0 86	350/0 86	350/0 86	350/0 86	350/0.86
CRITICAL FIELD/TO LENGTH FT	7500 x 86	7500 x 86	7500	8000	8000
LANDING LENGTH FT	5000	5000	5000	5500	5500
LCN	60	60	60	60	60
TURNING DEGREE	180 ON 90 FT	180 ON 90 FT		90 ON 75 FT FILLET	90 ON 75 FT FILLET
SUPPORT EQUIPMENT	SELF LAUNCH/CS	SELF LAUNCH/CS	SELF LAUNCH/CS	SELF LAUNCH/CS	SELF LAUNCH/CS
FLIGHT CREW	2 PILOTS	2 PILOTS	2 PILOTS	2 PIL+JUMPSEAT	2 PIL+JUMPSEAT
CARGO CREW	1 LM	2 LM OR JUMPMAST.	2 REFUEL OP STAT	2 LM	2 LM
AVIONICS	INT. FMS,NAV,DATAB	INT. FMS,NAV,DATAB	INT. FMS,NAV,DATAB	INT. FMS,NAV,DATAB	INT. FMS,NAV,DATAB
REST/RELIEF	UP TO 6 FLT CREW	UP TO 6 FLT CREW	UP TO 6 FLT CREW		
CARGO FLOOR HEIGHT IN	60-70	60-70	60-70		
PALLET ROLLERS	463L SYS. INTEGRAL	463L SYS. INTEGRAL	463L SYS. INTEGRAL		
RAMP ANGLE DEG MAX	12	12			
CREW DOORS IN	FWD PORT 32x48	FWD PORT 32x48	FWD PORT 32x48		
PARATROOP DOORS IN		2 36x72 FWD OF RMP			
AIRDROP-PERS. KIAS,FT(MIN)		130-135, 500-800			
AIRDROP-EQUIP. KIAS,FT(MIN)		150, 1000			
AIRDROP-CDS KIAS,FT(MIN)		150, 600			
AIRDROP-DR BUND KIAS,FT(MIN)		130-150, 300			
FUELING			SINGLE PT, PRESS.		
MAINT. MAN HR/FLIGHT HR	12	12	12		
DISPATCH RELIABILITY					
DESIGN LIFE FH	45,000	45,000	45,000		

TABLE 1

Appendix C

MATLAB File For Computing Structural and Aerodynamic Parameters

```
clear;
scale=0.5; % ratio of AFW wing span to empirical model 1081.2/700%
% stringer areas %
stringertoptip=0.53*scale;
stringertoproot=0.53*2*scale;
stringerbottip=0.43*scale;
stringerbotroot=0.43*2*scale;
% spar cap areas %
spartopfortip=0.5*scale;
spartopforroot=16.0*scale;
sparbotfortip=0.5*scale;
sparbotforroot=17.0*scale;
spartopafttip=0.5*scale;
spartopaftroot=15.0*scale;
sparbotafttip=0.5*scale;
sparbotaftroot=50.0*scale;
% skin thicknesses %
topskinroot=0.500*scale;
botskinroot=0.500*scale;
topskintip=0.050*scale;
botskintip=0.050*scale;
% other variables %
span=108.34*12;
E=1.05e7;
G=4.0e6;
density=.101;% pounds per cubic inch %
frontspar=.1369;
rearspar=.6251;

% set spanwise stations %
s=[3000
0
179.35
233.16
233.16
331.82
411.61
481.34
636.77
789.24
874.71
874.71
941.71
965.81
965.81
1094.18
1193.79
1193.79
1246.65
1300.12];
```

```
M(:,1)=s/1000;

s2=[0
179.35
233.16
331.82
411.61
481.34
636.77
789.24
874.71
941.71
965.81
1094.18
1193.79
1246.65
1300.12];

% chord values at each of the stations along the span %
c=[200
298.87
270.00
261.32
261.32
245.43
232.58
221.35
196.32
171.76
157.99
157.99
147.20
143.32
143.32
122.64
106.60
106.60
98.08
89.47];
M(:,2)=c/100;

c2=[0
298.87
270.00
261.32
245.43
232.58
221.35
196.32
171.76
157.99
147.20
143.32
122.64
106.60
98.08
89.47];

% alpha %
for w=2:length(s),
alpha(w,1)=3.5;
end
alpha(1,1)=1;
M(:,3)=alpha;
```

```
%determine twist%
twist(1,1)=1;
for w=2:length(s),
   twist(w,1)=2-3*s(w,1)/span;
end
M(:,11)=twist;

% determine sectional dimensions %
   % spar cap areas %
   for w=2:length(s),
        spartopfor(w,1)=spartopforroot-(spartopforroot-spartopfortip)*s(w,1)/span;
        spartopaft(w,1)=spartopaftroot-(spartopaftroot-spartopafttip)*s(w,1)/span;
        sparbotfor(w,1)=sparbotforroot-(sparbotforroot-sparbotfortip)*s(w,1)/span;
        sparbotaft(w,1)=sparbotaftroot-(sparbotaftroot-sparbotafttip)*s(w,1)/span;
   end
   % skin thicknesses %
   for w=2:length(s),
        topskin(w,1)=topskinroot-(topskinroot-topskintip)*s(w,1)/span;
        botskin(w,1)=botskinroot-(botskinroot-botskintip)*s(w,1)/span;
   end
   % stringer thicknesses %
   for w=2:length(s),
        stringertop(w,1)=stringertoproot-(stringertoproot-stringertoptip)*s(w,1)/span;
        stringerbot(w,1)=stringerbotroot-(stringerbotroot-stringerbottip)*s(w,1)/span;
   end
   % other properties %
   for w=2:length(s),
        if s(w,1)<110
           toverc(w,1)=16.3/100;
        else
           toverc(w,1)=(16.3-4.6*(s(w,1)-128)/(span-128))/100;
        end
        foilheight(w,1)=0.09*c(w,1)*toverc(w,1)/.12;
        boxarea(w,1)=foilheight(w,1)*(rearspar-frontspar)*c(w,1);
        numstringers(w,1)=floor(c(w,1)/2/12);
        totaltoparea(w,1)=spartopfor(w,1)+spartopaft(w,1)+numstringers(w,1)*stringertop(w,
1)+                    c(w,1)*topskin(w,1)*(rearspar-frontspar);
        totalbotarea(w,1)=sparbotfor(w,1)+sparbotaft(w,1)+numstringers(w,1)*stringerbot(w,
1)+                    c(w,1)*botskin(w,1)*(rearspar-frontspar);
        ct(w,1)=totalbotarea(w,1)*foilheight(w,1)/(totaltoparea(w,1)+totalbotarea(w,1));
        cb(w,1)=totaltoparea(w,1)*foilheight(w,1)/(totaltoparea(w,1)+totalbotarea(w,1));
                % sum moments and areas of stringers (stringers have 12 inch spacing) %
                sumaxstr(w,1)=0;
                sumax2str(w,1)=0;
                sumaxzstr(w,1)=0;
                sumastr(w,1)=0;
                sumaxskin(w,1)=0;
                sumax2skin(w,1)=0;
                sumaxzskin(w,1)=0;
                sumaskin(w,1)=0;
                sumaxspar(w,1)=0;
                sumax2spar(w,1)=0;
                sumaxzspar(w,1)=0;
                sumaspar(w,1)=0;
                for v=1:numstringers(w,1),
                   x=rearspar*c(w,1)-12*v;
                   sumaxstr(w,1)=sumaxstr(w,1)+(stringertop(w,1)+stringerbot(w,1))*x;
                   sumax2str(w,1)=sumax2str(w,1)+(stringertop(w,1)+stringerbot(w,1))*x^2;
                   sumaxzstr(w,1)=sumaxzstr(w,1)+stringertop(w,1)*x*foilheight(w,1);
                   sumastr(w,1)=sumastr(w,1)+stringertop(w,1)+stringerbot(w,1);
                end
                % sum moments and areas of skin %
                sumaxskin(w,1)=(rearspar^2-frontspar^2)/2*c(w,1)^2*(topskin(w,1)+botskin(w
```

```
,1));
                sumax2skin(w,1)=(rearspar^3-frontspar^3)/3*c(w,1)^3*(topskin(w,1)+botski
w,1));
                sumaxzskin(w,1)=(botskin(w,1)^2)*((rearspar^2-frontspar^2)*c(w,1))^2/4+(
ilheight                    (w,1)^2-(foilheight(w,1)-topskin(w,1))^2)*(rearspar^2-fron
par^2)*c(w,1)^2/4;
                sumaskin(w,1)=(rearspar-frontspar)*c(w,1)*(topskin(w,1)+botskin(w,1));
                % sum moments and areas of spar %
                sumaxspar(w,1)=(spartopfor(w,1)+sparbotfor(w,1))*frontspar*c(w,1)+(spart
aft                         (w,1)+sparbotaft(w,1))*rearspar*c(w,1);
                sumaxzspar(w,1)=(spartopfor(w,1)*frontspar*c(w,1)*foilheight(w,1)+sparto
ft(w,1)*rearspar*c(w,1)*foilheight(w,1));
                sumax2spar(w,1)=(spartopfor(w,1)+sparbotfor(w,1))*(frontspar*c(w,1))^2-
                            (spartopaft(w,1)+sparbotaft(w,1))*(rearspar*c(w,1))^2;
                sumaspar(w,1)=spartopfor(w,1)+sparbotfor(w,1)+spartopaft(w,1)+sparbotaft
,1);
                xcentroid(w,1)=(sumaxstr(w,1)+sumaxskin(w,1)+sumaxspar(w,1))/(sumastr(w,
+                           sumaskin(w,1)+sumaspar(w,1));
   end

% bending moments of inertia %
for w=2:length(s),
   Izz(w,1)=(totaltoparea(w,1)*ct(w,1)^2+totalbotarea(w,1)*cb(w,1)^2);
   Ixx(w,1)=abs((sumax2str(w,1)+sumax2skin(w,1)+sumax2spar(w,1))-(sumastr(w,1)+sumaskin(
1)+             sumaspar(w,1))*xcentroid(w,1)^2);
   Ixz(w,1)=abs((sumaxzstr(w,1)+sumaxzskin(w,1)+sumaxzspar(w,1))-(sumastr(w,1)+
            sumaskin(w,1)+sumaspar(w,1))*xcentroid(w,1)*cb(w,1));
end

% torsional moment of inertia %
for w=2:length(s),
   J(w,1)=4*boxarea(w,1)^2/((c(w,1)*(rearspar-frontspar)/topskin(w,1)+c(w,1)*(rearspar-
          frontspar)/botskin(w,1)));
end

% bending stiffness coefficient %
M(1,4)=floor(real(log10(Izz(2,1)*E)));
M(1,5)=floor(real(log10(Ixx(2,1)*E)));
M(1,6)=floor(real(log10(Ixz(2,1)*E)));
for w=2:length(s),
   EInn(w,1)=Izz(w,1)*E/10^(M(1,4));
   EIcc(w,1)=Ixx(w,1)*E/10^(M(1,5));
   EIcn(w,1)=Ixz(w,1)*E/10^(M(1,6));
end
M(:,4)=EInn;
M(:,5)=EIcc;
M(:,6)=EIcn;
M(1,4)=floor(real(log10(Izz(2,1)*E)));
M(1,5)=floor(real(log10(Ixx(2,1)*E)));
M(1,6)=floor(real(log10(Ixz(2,1)*E)));
EIcnscale=M(2,6)/4.3825

% torsional stiffness coefficient %
M(1,7)=floor(real(log10(J(2,1)*G)));
for w=2:length(s),
   GJ(w,1)=J(w,1)*G/10^(M(1,7));
end
M(:,7)=GJ;
M(1,7)=floor(real(log10(J(2,1)*G)));

% no-load deflection (degrees) %
for w=2:length(s),
    defl(w,1)=0-(w-1)/(length(s)-1);
end
```

```
% sweep deflection %
for w=2:length(s),
    swdefl(w,1)=sin(37/180*3.14159)*s(w,1);
end

% X(s) and Z(s) %
X=[200
0
99.398
129.19
129.19
183.821
228.0
266.6
352.67
437.08
484.41
484.41
521.5
534.85
534.85
605.93
661.07
661.07
690.32
719.95];

Z=[20
0
-4.237
-5.847
-5.847
-8.80
-11.19
-13.28
-17.93
-22.49
-25.05
-25.05
-27.05
-27.77
-27.77
-31.62
-34.60
-34.60
-36.26
-37.779];

M(:,9)=X/100;
M(:,10)=Z/10;

% Cea-Cle(s) %
CeaminusCle(1,1)=1;
for w=2:length(s),
    CeaminusCle(w,1)=.382;
end
M(:,12)=CeaminusCle;
M(1,12)=1;

% aerodynamic values %
dCloverDf(1,1)=1;
dCmoverDf(1,1)=1;
dCloverDa(1,1)=1;
```

```
dCmoverDa(1,1)=1;
for w=1:length(s),
        dCloverDf(w,1)=.291*s(w,1)/span;
        dCmoverDf(w,1)=-.0133*s(w,1)/span;
end
for w=14:16,
        dCloverDa(w,1)=.232;
        dCmoverDa(w,1)=-.0146;
end
for w=17:length(s),
        dCloverDf(w,1)=0;
        dCmoverDf(w,1)=0;
        dCloverDa(w,1)=0;
        dCmoverDa(w,1)=0;
end
M(:,13)=dCloverDf;
M(:,14)=dCmoverDf;
M(:,15)=dCloverDa;
M(:,16)=dCmoverDa;

% wing total weight = 20,621 lb %
% torque box mass =12,363 lb %
for w=2:length(s),
        B(w,1)=2.92*.37*4/c(w,1)^2*density/E/(toverc(w,1))^2;
        BEI(w,1)=B(w,1)*EIcc(w,1)*10^11;
end

% leading edge mass %
for w=2:length(s),
        Mle(w,1)=c(w,1)*1030/252421;
end

% trailing edge mass %
for w=2:length(s),
        Mte(w,1)=c(w,1)*7212/(298.87+89.47)*2/1300.1;
end

totalfuelweight=0;
% fuel mass %
for w=2:16,
        Mf(w,1)=c(w,1)^2*toverc(w,1)*114931/7850027/2;
end
for w=17:length(s),
        Mf(w,1)=0;
end

% total weight distribution %
M(1,8)=floor(real(log10(Mle(2,1)+Mte(2,1)+Mf(2,1))));
for w=2:length(s),
        MG(w,1)=(Mle(w,1)+Mte(w,1)+Mf(w,1)+BEI(w,1))/10^(M(1,8));
end
M(:,8)=MG;
M(1,8)=floor(real(log10(Mle(2,1)+Mte(2,1)+Mf(2,1))));
MGscale=MG(2,1)/1.3109

% center of gravity %
for w=2:length(s),
     Xcg(w,1)=(Mf(w,1)*.4+BEI(w,1)*.382+Mle(w,1)*.075+Mte(w,1)*.825)/MG(w,1);
end
```

Appendix D

ASWING Input File

```
Name
AFW
End
!
Units
L 0.083333 ft
T 1.0 s
F 1.0 lb
End
!
                chord     alpha       EIcc      EInn       EIcn       GJ
*      1e3        1e2         1       1e11       1e12       1e11     1e11
         0     2.9887    3.5000     9.2063     8.4224     4.3825   7.7912
    0.1793     2.7000    3.5000     6.0269     5.7881     3.0300   4.9076
    0.2332     2.6132    3.5000     5.1283     5.0569     2.6284   4.1490
    0.3318     2.4543    3.5000     3.8271     4.0436     2.0704   3.0053
    0.4116     2.3258    3.5000     2.9460     3.2604     1.6490   2.2792
    0.4813     2.2135    3.5000     2.3422     2.7267     1.3621   1.7666
    0.6368     1.9632    3.5000     1.3230     1.7108     0.8295   0.9508
    0.7892     1.7176    3.5000     0.6965     1.0008     0.4681   0.4742
    0.8747     1.5799    3.5000     0.4598     0.6939     0.3168   0.3054
    0.9417     1.4720    3.5000     0.3267     0.5213     0.2322   0.2095
    0.9658     1.4332    3.5000     0.2802     0.4456     0.1966   0.1814
    1.0942     1.2264    3.5000     0.1271     0.2225     0.0911   0.0769
    1.1938     1.0660    3.5000     0.0561     0.0988     0.0353   0.0339
    1.2467     0.9808    3.5000     0.0331     0.0580     0.0166   0.0201
    1.3001     0.8947    3.5000     0.0149     0.0203     0.0003   0.0108
!--------------------
          Cm      Cd
* 1e3     1.0   1.0
0.0     -0.15   0.01
1.3001  -0.15   0.01
!--------------------
              mg         x         z        t         Xea        Xcg      Atshell
*     1e3     1e2       1e2       1e1        2         1          1        1e-5
         0  1.3109         0         0   2.0000    0.3820     0.409    4.6529
    0.1793  1.0746    0.9940   -0.4237   1.5861    0.3820     0.409    4.5777
    0.2332  1.0015    1.2919   -0.5847   1.4620    0.3820     0.409    4.5120
    0.3318  0.8798    1.8382   -0.8800   1.2343    0.3820     0.409    4.3905
    0.4116  0.7860    2.2800   -1.1190   1.0502    0.3820     0.409    4.2915
    0.4813  0.7112    2.6660   -1.3280   0.8893    0.3820     0.409    4.2043
    0.6368  0.5578    3.5267   -1.7930   0.5306    0.3820     0.409    4.0075
    0.7892  0.4271    4.3708   -2.2490   0.1788    0.3820     0.409    3.8098
    0.8747  0.3605    4.8441   -2.5050  -0.0184    0.3820     0.409    3.6963
    0.9417  0.3142    5.2150   -2.7050  -0.1730    0.3820     0.409    3.6052
    1.0942  0.2171    6.0593   -3.1620  -0.5249    0.3820     0.409    3.3895
    1.0942  0.2171    6.0593   -3.1620  -0.5249    0.3820     0.549    3.3895
    1.1938  0.0594    6.6107   -3.4600  -0.7547    0.3820     0.549    3.2387
    1.2467  0.0497    6.9032   -3.6260  -0.8767    0.3820     0.553    3.1543
    1.3001  0.0369    7.1995   -3.7779  -1.0001    0.3820     0.562    3.0641
!--------------------
              dCLdA      dCMdA
```

```
*       1e3         1          1
          0         0          0
     0.9658         0          0
     0.9658    0.0730    -0.0100
     1.1938    0.0730    -0.0100
     1.1938         0          0
     1.3001         0          0
!--------------------
                 dCLdF        dCMdF
*       1e3          1          1
          0          0          0
     1.3001      0.110    -0.0100
!--------------------
              CLmax    CLmin     dCLda    Cshell  Nshell
*    1e3        1        1         1         1       1
    0.0       1.5      -1.13     6.29      0.25    0.08
    1.3001    1.5      -1.13     6.29      0.25    0.06
!======================
weight
!!!  s        dC       dS        dN        Mg
*    1e3        1        1         1      1000.0
    0.411    -198.80  -93.03   -80.945     15
end
```

References

[1] Norris M., and J. Miller, "Active Flexible Wing Technology Assessment Study," Lockheed Aeronautical Systems, Marietta, Georgia, 1994

[2] Numerous Articles in Journal of Aircraft, Published Bimonthly by: American Institute of Aeronautics and Astronautics, 370 L'Enfant Promenade, SW, Washington DC 20024. (Issue used: Feb. 1995)

[3] Boppe C., "System Requirement Types," Class Lecture Notes, Course 16.870, Massachusetts Institute of Technology, Cambridge MA, Fall, 1995.

[4] Roskam, J., "Airplane Design: Part VIII: Airplane Cost Estimation: Design, Development, Manufacturing, and Operating," Roskam Aviation and Engineering Corporation, Rt4, Box 274, Ottawa, KS 66067.

[5] Wohletz, J., Hesse, C., and et al, AE 522, Spring 1994, "Preliminary Design of the Avocet: A Low Cost Commercial Transport," University of Kansas, Lawrence, KS, 66045.

[6] Boppe, C., "QFD-Quality Functional Deployment," Class Lecture Notes, Course 16.870, Massachusetts Institute of Technology, Cambridge, MA, Fall, 1995.

[7] MIL-A-88618 Amendment 1 December 5, 1994

[8] Nui, "Aircraft Structural Design," Unknown Publisher.

[9] Ewing, M., "Aerospace Structures," Custom Academic Publishing Company, 913 North Broadway, Oklahoma City, OK, 1995

[10] Taylor, J.W.R., Jane's All the World's Aircraft: Published Annually by: Jane's Publishing Company. 238 City Road, London EC1V 2PU, England. (Issue used: 1995/ 96)

[11] Preliminary Design Methods Group, "The ACAD User's Manual," Lockheed Martin Corporation, April 1995.

[12] Wohletz, J., Master's Thesis (in progress), Massachusetts Institute of Technology, Cambridge, MA.

[13] Neill, D.J., and D.L. Herendeen, "Volume 1- ASTROS User's Manual," Flight Dynamics Directorate, Wright Laboratory, Air Force Materiel Command, Wright-Patterson Air Force Base, OH 45433, March 1993.

[14] Drela, M., "ASWING User's Guide," Massachusetts Institute of Technology, Cambridge, MA, 1990.

[15] Drela, M., Personal Communication, Massachusetts Institute of Technology, Cambridge, MA, 5/9/96.